NASA Contractor Report 178056

FURTHER INVESTIGATION INTO CALIBRATION TECHNIQUES FOR A MAGNETIC SUSPENSION AND BALANCE SYSTEM

J. Eskins

THE UNIVERSITY OF SOUTHAMPTON
Southampton, England

NASA

National Aeronautics and
Space Administration

Langley Research Center
Hampton, Virginia 23665

List of Symbols

F_x - Fz forces acting on the model

g acceleration due to gravity

I_j current in the jth electromagnet

I_{jk} current in the jth electromagnet when mass, m_k, is attached to the model

I_{Lk} summed lift current when mass, m_k, is attached to the model

I_D drag current, i.e. summation of the currents in the electromagnets providing drag force

I_L lift current, i.e. summation of the currents in the electromagnets providing lift force

I_P pitch current, i.e. summation of the currents in the electromagnets providing pitching moment

I_S current in superconducting solenoid

I_L' mean summed lift current for a dynamic oscillation

K_{ij} calibration constant for the ith degree of freedom and jth electromagnet

K_i calibration constant for the ith degree of freedom (current providing this force/moment being summed)

K_3' z-direction calibration constant per unit solenoid current

k_1 inner core/outer can stiffness factor

k_2 core to ground stiffness (a magnetic stiffness)

L, M, N moments acting on the model

m mass of the model

m_1 mass of outer can (superconducting solenoid model)

m_2 mass of inner core (superconducting solenoid model)

m_k mass added to the model to apply a static force or model

t time

x, y, z tunnel axes

x', y', z' translated model axes

x'', y'', z'' translated and rotated model axes

z_m centreline of position trace during a dynamic lift oscillation

ψ, θ, ϕ yaw, pitch and roll of the model

ϕ_L current phase

ϕ_z position phase

ω angular frequency

1   INTRODUCTION

Magnetic Suspension and Balance Systems (MSBS) for wind tunnels offer many advantages over conventional supports.

The major advantage is :-

   a) Elimination of sting interference with no modification of the model to accommodate the sting

but others include,

   b) Ease of model movement allowing dynamic testing

   c) Fast, efficient testing at almost any attitude

   d) The type of model suspended can be changed without alterations in the support systems.

To take full advantage of the inherent attributes of MSBS a standard calibration technique should be developed. For instance, if a model was changed, but the magnetic core were standard, the whole support system need not be re-calibrated. However, without mechanical supports between the model and the tunnel, force/moment calibration of the system is not straightforward. This report investigates the relationship between the forces and moments applied to a magnetically suspended model and the currents in the electromagnet array. The disadvantage of this technique is that the calibration is performed in the wind tunnel. This wastes tunnel time and for a large MSBS (LMSBS) would be costly. A method to reduce the calibration time to a minimum is essential.

Previously most of the calibration of models in SUMSBS was carried out statically. This is achieved by applying known forces and moments, using weights and pulleys, and monitoring the currents in the electromagnet array. For a LMSBS this would be clumsy as well as costly and time-consuming.

An alternative approach to static calibration is dynamic calibration. This involves oscillating a model in a particular mode (e.g pitch), recording its motion, in addition to the electromagnet currents, and using the model's inertia to calibrate the system. Previous work[1,2] has shown this to be a promising calibration method. In principle dynamic calibration can calibrate all degrees of freedom, for a large range of attitudes, in a very short time.

A major cost of LMSBS is the building and running of the electromagnet array. The physical size of the electromagnets and running costs can be reduced considerably by using superconducting magnets. A major saving can be made by increasing the magnetic moment of the model. For conventional

1

cores there is a limit to the magnetic moment per unit volume, but using a superconducting solenoid[1] to provide the magnetic field the magnetic moment is dependent on the solenoid current. For large models, although there is a limit to the solenoid current, the magnetic moment per unit volume of model can be made greater for a superconducting model than the best permanent magnetic material.

A pilot model was built and flown at Southampton in July 1983[1] and again in May 1984. Data from the later tests on this model is included here together with calibration work on conventional cores.

2   CALIBRATION THEORY

In general the model can be treated as being acted upon by three orthogonal forces and three moments (see Figure 1). SUMSBS uses ten electromagnets to produce the required orientation, with some redundancy therefore in the electromagnet array.

The force/moment balance can be represented as (1).

$$
\begin{bmatrix} F_x \\ F_y \\ F_z \\ L \\ M \\ N \end{bmatrix} = \begin{bmatrix} K_{ij} \end{bmatrix} \begin{bmatrix} I_1 \\ I_2 \\ I_3 \\ \cdot \\ \cdot \\ \cdot \\ \cdot \\ \cdot \\ I_9 \\ I_{10} \end{bmatrix} \tag{1}
$$

The purpose of the calibration is to determine the elements in the array K_{ij}. There is a further complication in that the matrix K_{ij} is a function of model position and attitude, (see Figure 1) i.e

$$
K_{ij} = K_{ij}(x, y, z, \psi, \theta, \phi)
$$

K_{ij} is also a function of the magnetic moment of the model. In particular for the superconducting model, K_{ij} will be a function of solenoid current.

2

This method of calibration involves subjecting a model to one or more forces and moments (F_x - N) and monitoring the currents required to hold the model at the required orientation. A method of least squares can then be used to determine elements in K_{ij}.

There are special cases where pure forces or moments are applied or only certain electromagnets contribute significantly to resisting the applied force or moment. This is true for calibrations described in this report, where tests took place with the model central, in position and attitude, in the wind tunnel. For this case lift force and pitching moment are produced only by the four electromagnets 1, 3, 7, 5 (Figure 1), and drag force affected only by the two axially wound coils, 9 and 10. This can be expressed from equation (1) as :-

$$F_z = K_{31} I_1 + K_{33} I_3 + K_{35} I_5 + K_{37} I_7 \tag{2}$$

with

$$K_{32} = K_{34} = K_{36} = K_{38} = K_{39} = K_{3,10} = 0$$

$$M = K_{51} I_1 + K_{53} I_3 + K_{55} I_5 + K_{57} I_7 \tag{3}$$

with

$$K_{52} = K_{54} = K_{56} = K_{58} = K_{59} = K_{5,10} = 0$$

$$F_x = K_{19} I_9 + K_{1,10} I_{10} \tag{4}$$

with

$$K_{11} = K_{12} = K_{13} = K_{14} = K_{15} = K_{16} = K_{17} = K_{18} = 0$$

In the past equations 2, 3, 4 have been further simplified by assuming the magnitude of the contribution of each coil, to the total force or moment, to be the same, giving

$$F_z = K_3 (I_1 + I_3 + I_5 + I_7) = K_3 I_L \tag{5}$$

$$M = K_5 (I_1 + I_3 - I_5 - I_7) = K_5 I_p$$

$$F_x = K_1 (I_9 + I_{10}) = K_1 I_D$$

3

Static calibration involves the application of known forces and torques F_x - N. A static lift force (F_Z)calibration can be represented as

$$(m_k + m)g = K_{31} I_{1k} + K_{33} I_{3k} + K_{35} I_{5k} + K_{37} I_{7k} \qquad (8)$$

or

$$(m_k + m)g = K_3 I_{Lk} \qquad (9)$$

At least four readings are needed to solve (8), sensibly many more, by a least squares method. K_3 in equation (9) can be found from the gradient of lift current, I_L against added weight $m_k g$. Static calibration for pitching moment and drag force can be analysed in a similar way using (6) and (7).

Dynamic calibrations involve using the model's own inertia to calibrate the suspension system. For instance, using (5), oscillations in the z-direction, which could be induced with a view to determining a lift force calibration, can be represented as

$$mg + m\ddot{z} = K_3 I_L(t)$$

For sinusoidal motion

$$z(t) = z_m + z e^{i(\omega t + \phi_z)}$$

$$\ddot{z} = -\omega^2 z e^{i(\omega t + \phi_z)}$$

fitting a sinusoid to the current

$$I_L(t) = I_L' + I_L e^{i(\omega t + \phi_C)}$$

gives

$$\textit{static} \qquad mg = K_3 I_L'$$

$$\textit{dynamic} \qquad -m\omega^2 z = K_3 I_L e^{i(\phi_C - \phi_z)}$$

Taking the real part of the dynamic component

$$-m\omega^2 z = K_3 I_L \cos(\phi_C - \phi_z) \qquad (10)$$

Previous analysis [1,2] did not take account of phase angles, by assuming no damping and simple harmonic motion with $\phi_C - \phi_z = 180°$, giving

$$m\omega^2 = K_3 \frac{I_L}{z} \tag{11}$$

For a range of frequencies and amplitudes a graph of I_L/z against ω^2 should be a straight line with gradient m/K_3.

If it is found that phase shifts are present a more general equation for the motion including damping and stiffness terms could be represented as below

$$F_z(t) = mz + cz + kz \tag{12}$$

An analysis similar to above gives

$$m\omega^2 - k = -K_3 \frac{I_L}{z} cos(\phi_C - \phi_z) \tag{13}$$

- a plot of $-\frac{I_L}{z} cos(\phi_C - \phi_z)$ against ω^2

should be a straight line with gradient m/K_3

The same analysis could be applied to all other modes of oscillation to yield similar results.

For the superconducting model, a lift constant, K_3, was found for solenoid currents of 10A, 15A and 20A. The magnetic moment of the model is directly proportional to the solenoid current, I_s implying

$$F_z = K_3' I_L I_s \tag{14}$$

The lift constant found by experiment, K_3, is given by

$$K_3 = K_3' I_s$$

where K_3' will be a constant for this configuration at a central position.

A graph of K_3 against solenoid current, I_s, should be linear.

3 CALIBRATION PROCEDURE

3.1 Superconducting Solenoid model

The superconducting solenoid model (see Figure 2) is much larger than conventional models flown in SUMSBS and for this reason in previous testing[1] had been flown 'high', that is with the model suspended well above the wind tunnel's centreline.   This feature had produced some unsatisfactory results. To suspend the model centrally in the tunnel,the paths of the four light beams detecting y, z, m, n motions were diverted using ordinary mirrors mounted to form small periscopes. Restraining rings were mounted in the tunnel to protect the model and tunnel in the event of loss of control. The rings also served as a convenient launch pad during launching.

Several software changes were made to the existing program before the model was flown. Gains were altered according to calculations, to allow for the different magnetic moment of the model[1], compared to those normally suspended. Provision for real-time gain selection was included to optimise the calculated gains. For convenience extra keyboard commands such as "switch-off current output" and "reverse current polarity" were included. It was decided to test some devices on the model for providing roll torque[4]. Software changes were made so that, using a keyboard command, the current in electromagnets 1 – 8 could be incremented symmetrically to produce pure rolling moment only in addition to their usual functions. To accommodate these new keyboard commands the character array size was increased.

Preliminary experiments were performed with the roll current components commanded and a dummy model flying. These showed no instability in control. Initial tests with the roll device mechanically suspended, gave promising roll torque. These devices were tested whilst mounted to the superconducting model in flight. The results of this work are detailed in Reference 4.

The majority of testing on the superconducting model was at a solenoid current of 15A, but some work was carried out at solenoid currents of 10A and 20A.

3.1.1   Static calibration with the Superconducting Solenoid model

Static calibration was performed by applying known weights to the model. This was achieved for drag force (F_x), in the negative x-

direction of Figure 1, using a pulley system attached to the rear of the model. and for lift force and pitching moment (F_z, M) by hanging these weights at fore and aft stations on the model. Examples of static lift calibrations at solenoid currents of 15A and 10A are shown in Figures 3,4. A drag calibration at a solenoid current of 15A is shown in Figure 5. In the pitching moment calibrations a pure torque could not easily be applied to the model so a combined force and moment was applied. This calibration was further complicated by the fact that the magnetic centre of force and centre of gravity did not coincide and merely suspending the model produces a pitching moment about the model's centre of gravity, that needs to be resisted by electromagnet currents. Further calibration weights added increase this "suspension moment". These effects were compensated for and Figures 6,7 show the true pitch calibration at solenoid currents of 15A and 10A.

Three lift calibration constants were found for solenoid currents of 10A, 15A and 20A. The variation of lift constant with solenoid current is shown in Figure 8.

3.1.2 Dynamic calibrations with the Superconducting Solenoid model

Before these calibrations were performed it was necessary to calibrate the optical system which is used to monitor the motion of the model. For this purpose a cylinder, the same diameter as the model, was moved incrementally with a vernier traverser through the optical system light beams in the z-direction. All data, including the signals from the optical system, were logged into the computer through a 12-bit A/D converter. A typical optical system calibration with fitted curve is shown in Figure 9.

For dynamic oscillations, keyboard commands were used to select the mode of oscillation, the motion amplitude and frequencies ranging from 34 rad/s to 101 rad/s. The model was oscillated in lift (z-direction) for solenoid currents of 10A, 15A and 20A. The data which were recorded during oscillations included all electromagnet currents and the model's position signals. Examples of these oscillations with fitted sine-curves are shown in Figures 10 to 14. Pitch oscillations at 15A and 10A are shown in Figures 15 and 16. This work is analysed and compared with static results in Section 4.

3.2 Conventional Models

Similar procedures were used in the static and dynamic calibration of permanent magnet models. Two types of model core were used, the usual Alnico V core and a samarium cobalt core, which has a larger resistance to demagnetization. Static lift calibrations were performed using brass rings fitted around the model. During these calibrations some data were taken with one of the four lift electromagnets switched off. Using these results four separate calibrations constants for each lift coil could be extracted. These are compared with the results obtained from the static lift calibration plots of Figures 17, 18 in Section 4.

Dynamic lift calibrations were performed on both models over a frequency range of 18.4 rad/s to 165.7 rad/s. Sample oscillations with fitted curves are shown in Figures 19 to 22. Analysis of these traces is included in the next section.

4 DISCUSSION

4.1 Superconducting Model

The superconducting model was successful as a proof of concept prototype, proving reliable in all its original design functions. Although the model surpassed all expectations for its performance, it was not ideal for calibration work in the wind tunnel associated with SUMBS for the following reasons:-

(i) the model was too large

(ii) the magnetic centre of force and centre of gravity did not coincide

(iii) the core has some freedom of movement within the outer can

4.2 Static Calibrations

Static data taken with the superconducting model seemed to be accurate and showed the good linearity that had been experienced previously with permanent magnet models.

The experiments with roll devices proved their feasibility for use with models without wings[4], an example of a calibration curve for the samarium cobalt roll device is shown in Figure 23.

Previously, the extrapolation back to zero lift current[1] of static lift calibration data for the superconducting model gave an indicated model mass approximately 700 grams (~40%) less than the true value. This was thought to be due to the off-centre line suspension (high) producing

8

attraction to the upper iron pole-piece. With the model suspended centrally, (see Figures 3,4), the extrapolation implies a model mass to within 1% of the half filled value (liquid helium boil off accounts for 1.4% of the total mass).

Good linearity is also shown for static lift calibrations performed on Alnico and samarium cobalt cores, Figures 17,18. There is a spread of data around zero applied mass, these points representing data taken with only three lift coils used to support the model. Using this data four separate lift constants were calculated for each model core as follows:-

	Alnico core			Samarium-Cobalt core	
K_{33}	= -0.0809	N/A	K_{33}	= -0.0577	N/A
K_{31}	= 0.0707	N/A	K_{31}	= 0.0532	N/A
K_{37}	= 0.0759	N/A	K_{37}	= 0.0566	N/A
K_{35}	= -0.0669	N/A	K_{35}	= -0.0512	N/A

compared with values of $K_3 = 0.0736$ N/A for Alnico and $K_3 = 0.055$ N/A for samarium cobalt. Each electromagnet is clearly not contributing the same lift force per unit current. Although the summed data (yielding K_3) are accurate when all four electromagnets are running, the approach is not as general as finding four separate constants. Separate calibration constants for each coil should, it is felt, be used more often.

Analysis of pitching moment calibration data for the superconducting model was complicated by the fact that pure torque was not applied to the model. Once this effect was compensated for, the pitching moment calibration data in Figures 6,7 showed good linearity.

Drag calibrations (e.g Figure 5) carried out on the superconducting solenoid were satisfactory.

Theory suggests that the lift constant for the superconducting model should be directly proportional to the solenoid current. The limited data available plotted on Figure 8 show this to be true.

4.3   Analysis of Dynamic Oscillations

Dynamic lift calibrations performed on the superconducting model[1] prior to this experiment produced some unsatisfactory waveforms. The model's position followed a sine-curve well but the current needed to produce this motion was distorted. This was thought at the time to be due to the attraction to the upper iron pole-pieces mentioned in Section 4.2.

9

The model was suspended centrally for all of the tests covered by this report, and none of the above distortion is apparent. In this experiment position data seemed to follow a sine-curve well (the model's motion is closed-loop controlled) but the current traces contain some noise, less apparent at the high frequencies, where the actual current signal is larger.

Dynamic oscillation data consisted of scans of data containing ten electromagnet currents, vertical motion fore and aft, and a reading of time for each scan.

During the course of analysis various improvements were made to the technique. For the superconducting model only the middle 15% of the vernier position calibration was needed because of restrictions on amplitude imposed by the containment rings. A straight line fit across the range of the position calibration was not appropriate since the data showed a slight curve. Therefore a least-squares cubic B-spline fit was used, as shown in Figure 9. Earlier analysis had relied on a control loop frequency of 400 Hz giving data points equally spaced 2.5 ms apart and oscillation frequencies as multiples of keyboard commands. With extra tasks included in the software the loop rate fell to around 375 Hz. Each data set had an independent reading of time from the internal clock of the computer and this was used to time the data points.

It was decided to use a general curve-fitting technique, fitting a curve of the form

$$y_i = A + B \sin(Ct_i + D)$$

where y_i is the motion or current reading and t_i is the corresponding time. This technique fits coefficients A, B, C and D where previously the practice had been to fit only A and B following the assumption of a known frequency of oscillation.

Dynamic calibration had been investigated earlier for permanent magnet models by Goodyer[2]. These experiments used a small band of frequencies and obtained results to within 2% of the corresponding static calibration. The experiments detailed by this report cover a wider range of frequency.

A graph of I_L/z cos(phase) against frequency squared for the superconducting model is shown in Figure 24. According to the theory presented in Section 2 this graph should be a straight line. As can be seen the data show a shallow curve of the form

$$(15)$$

$$y = a + bx + cx^2$$

where $x = w^2$, the frequency squared.

One attempt to explain the curve uses a representation of a tuned model[5]. The construction of the superconducting model allows it to be treated as an outer can separated from the inner solenoid by a spring/damper system. Ignoring some stiffness and damping factors[5] that are in the circumstances negligible and simplifying, terms a,b, c in equation (15) can be related to physical constants

$$a = k_2$$

$$b = (m_1 + m_2)/K_3$$

$$c = - \frac{m_1 m_2}{k_1 K_3}$$

The value of b found from the curve fit implies a dynamic lift constant, (at a solenoid current of 15A) of 1.27 N/A. The corresponding static value is 1.30 N/A, a 2.3% discrepancy. For a solenoid current of 20A the lift constant from dynamic calibration was within 2% of the static calibration value.

For pitch oscillations of the superconducting model a plot of I_P/ϕ cos(phase) against frequency squared at a solenoid current of 15A is shown in Figure 27. The moment of inertia of this model was found by bifilar suspension and later using a precision torsional pendulum. From the moment of inertia and the gradient of Figure 27 the pitch calibration constant was found to be 4% lower than that derived from a static calibration. The limited data available for Figure 27 show a linear calibration plot in contrast to the graph shown in Figure 24.

It must be realised the pilot superconducting model is an unconventional model to fly in the Southampton University MSBS. Apart from points (i), (ii) and (iii) (discussed in Section 4.1) effects such as

    a) liquid helium sloshing

    b) induced currents in the model's core

    c) aerodynamic damping

d) eddy currents in the framework

may be present. These effects have been assumed to be negligibly small or have been taken into account in the explanation of the curve of Figure 24 for superconducting model data. However some of the effects mentioned above could also apply to the dynamic calibration of models with conventional cores. Work prior to this [2] has not investigated dynamic lift calibration for conventional cores, over such a wide range of frequencies. For these reasons it was decided to repeat the tests over a broadened frequency band with Alnico and later samarium-cobalt cores.

The same analysis used previously was applied to the sine-fits for Alnico and samarium-cobalt data, this is shown in Figures 25, 26. Again according to simple theory these graphs should be straight lines. Figure 25 for Alnico data follows a curve similar to that of the superconducting model, but cannot be explained by the same argument of a "tuned model". The samarium cobalt data of Figure 26 show an S-shaped curve. Neither of the non-linear curves have yet been explained.

It may be argued that, since the model's position is controlled and therefore closely follows a sine-curve, more accurate results will be obtained where the current has a better fit as a result of a higher signal to noise ratio. This applies at the larger current amplitudes, but, where tests were repeated at the same frequency for two different amplitudes, one large and one small, no difference in the results was noticed.

A straight line fit over the low frequency portion of each curve yields some reasonable results. For Alnico a value of $K_3 = 0.0725$ N/A compared with 0.0736 N/A found statically. For samarium-cobalt $K_3 = 0.0549$ N/A compared with 0.0545 N/A in the static calibration.

As for the static calibration technique, the adding of the currents in the four electromagnets to produce one lift constant is not entirely satisfactory. Investigation showed that some coils were working harder than others during the dynamic calibrations. There was also a large phase difference between current and motion for samarium-cobalt data in the frequency band 75 rad/s to 125 rad/s of Figure 26. It is possible that there are other modes of oscillation being excited. For example an 'indicated' pure lift oscillation may in fact contain some other component of motion such as pitch or yaw due to faults such as non-linearity or misalignment in the light beams.

It is planned to install new position sensors which should be accurate and invariant and therefore eliminate some sources of error. Further study of dynamic calibration techniques is planned with an attempt to analyse the individual contributions of each electromagnet more fully. Fourier analysis on the waveforms may resolve questions on secondary oscillation modes and noise affecting traces. The new sensors will also enable high angles of attack to be monitored. With the aid of new software, a move will be made towards full calibration of the balance in all modes and over a wide range of attitudes. It is hoped in due course to secure an explanation the non-linearities highlighted above.

REFERENCES

1   Britcher, C.P.   Performance measurements of a Pilot Superconducting Solenoid model core for a Wind Tunnel MSBS. NASA-CR-172243, Nov. 1983.

2   Goodyer, M.J.   A preliminary Investigation of the Dynamic Force calibration of a Magnetic Suspension and Balance system. NASA-CR-172580, May 1985.

3   Wu, Y.Y.   Design of a horizontal liquid helium cryostat for refrigerating a flying superconducting magnet in a wind tunnel. NASA-CR-165980, August 1982.

4   Goodyer, M.J.   The generation of rolling moments with the superconducting solenoid model. NASA CR-172520, Jan. 1985.

5   Goodyer, M.J.   The Magnetic Suspension of Wind Tunnel models for Dynamic Testing. Univ. of Southampton, Dept. of Aeronautics & Astronautics - Ph.D Thesis, April 1968.

                     (Available as acquisition number N78-78589 for chapters 1-8 and N78-78219 for chapters 9-14.)
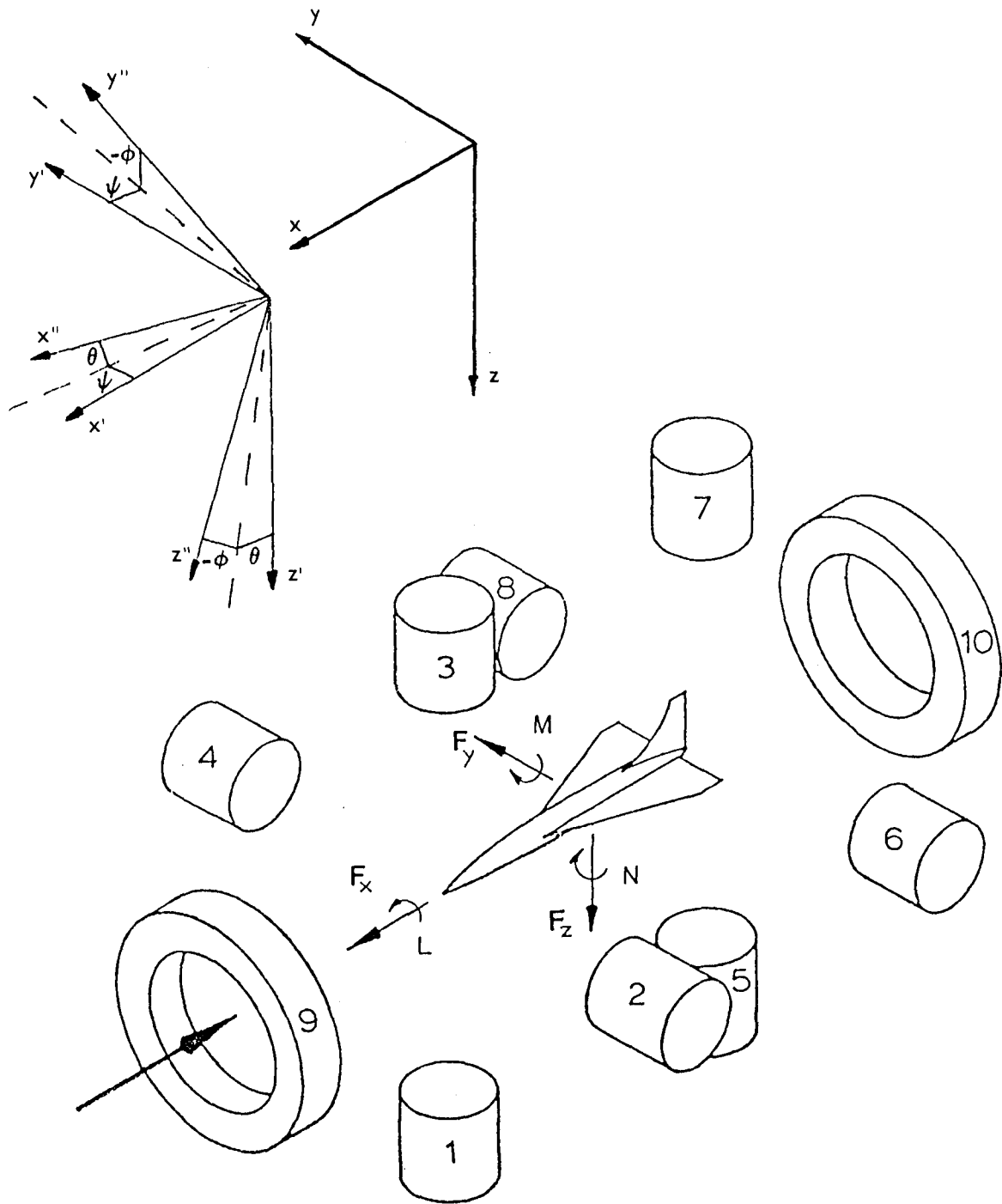
FIGURE 1. SCHEMATIC OF THE 6-COMPONENT MAGNETIC SUSPENSION AND BALANCE SYSTEM AT THE UNIVERSITY OF SOUTHAMPTON.

Fig. 2   CROSS SECTION OF THE SOUTHAMPTON UNIVERSITY PILOT SUPERCONDUCTING MODEL
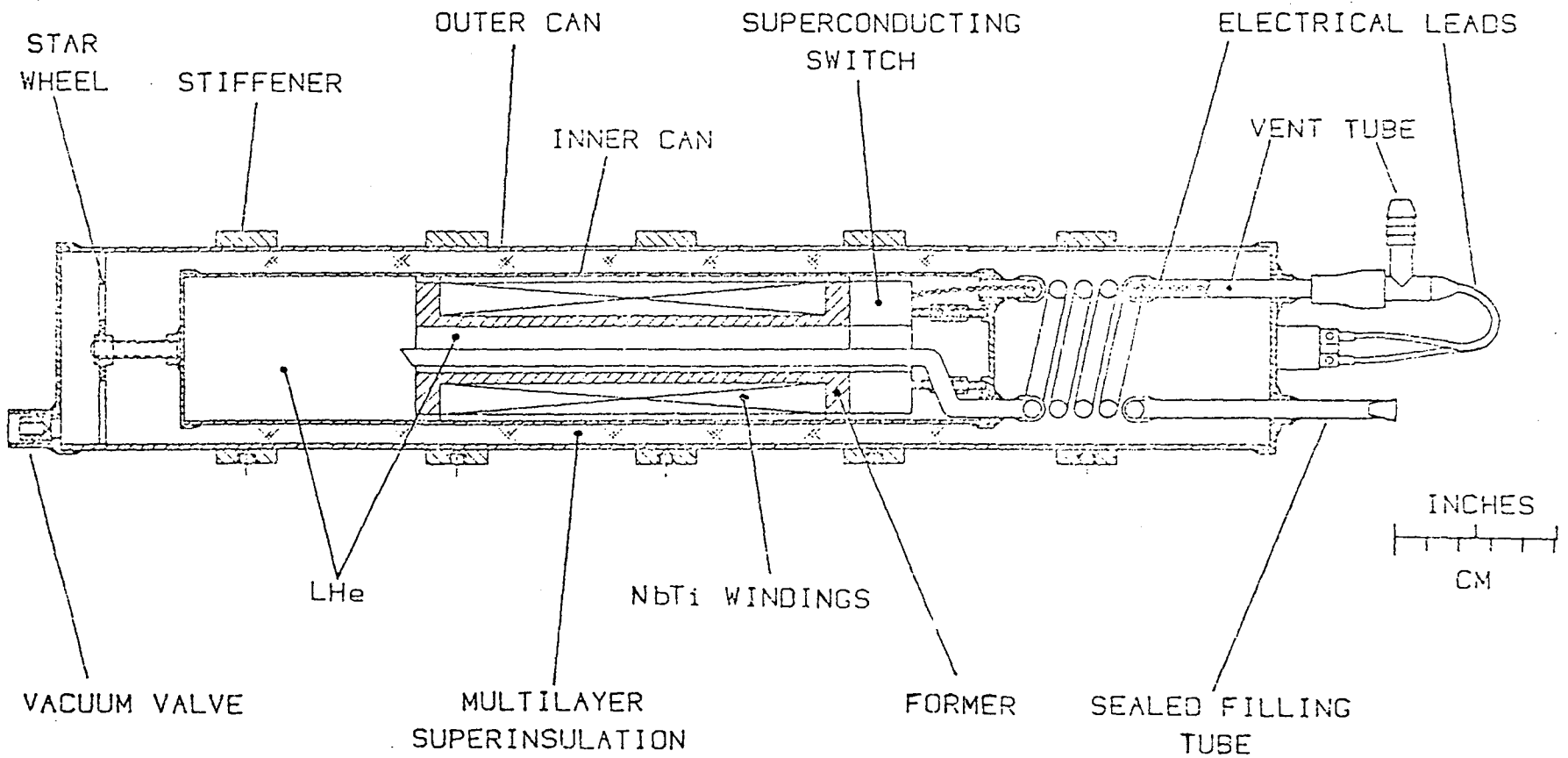
16

Fig.3   STATIC LIFT CALIBRATION (SOLENOID CURRENT @ 15A)

GRADIENT = .771 A/N

INTERCEPT ON Y-AXIS = 13.818 A

Fig.4   STATIC LIFT CALIBRATION (SOLENOID CURRENT @10A)

GRADIENT = 1.15 A/N

INTERCEPT ON Y-AXIS = 20.55 A

18
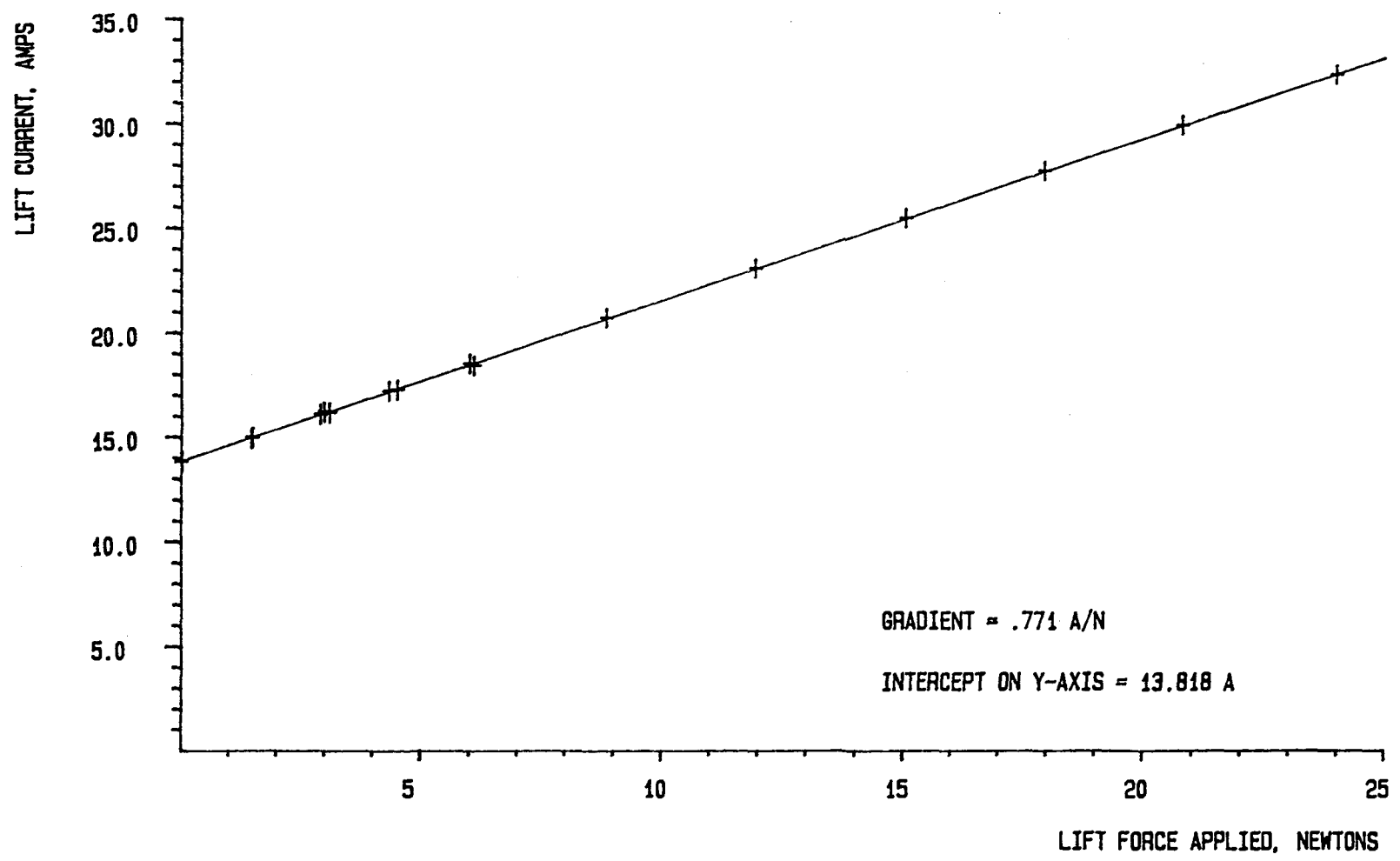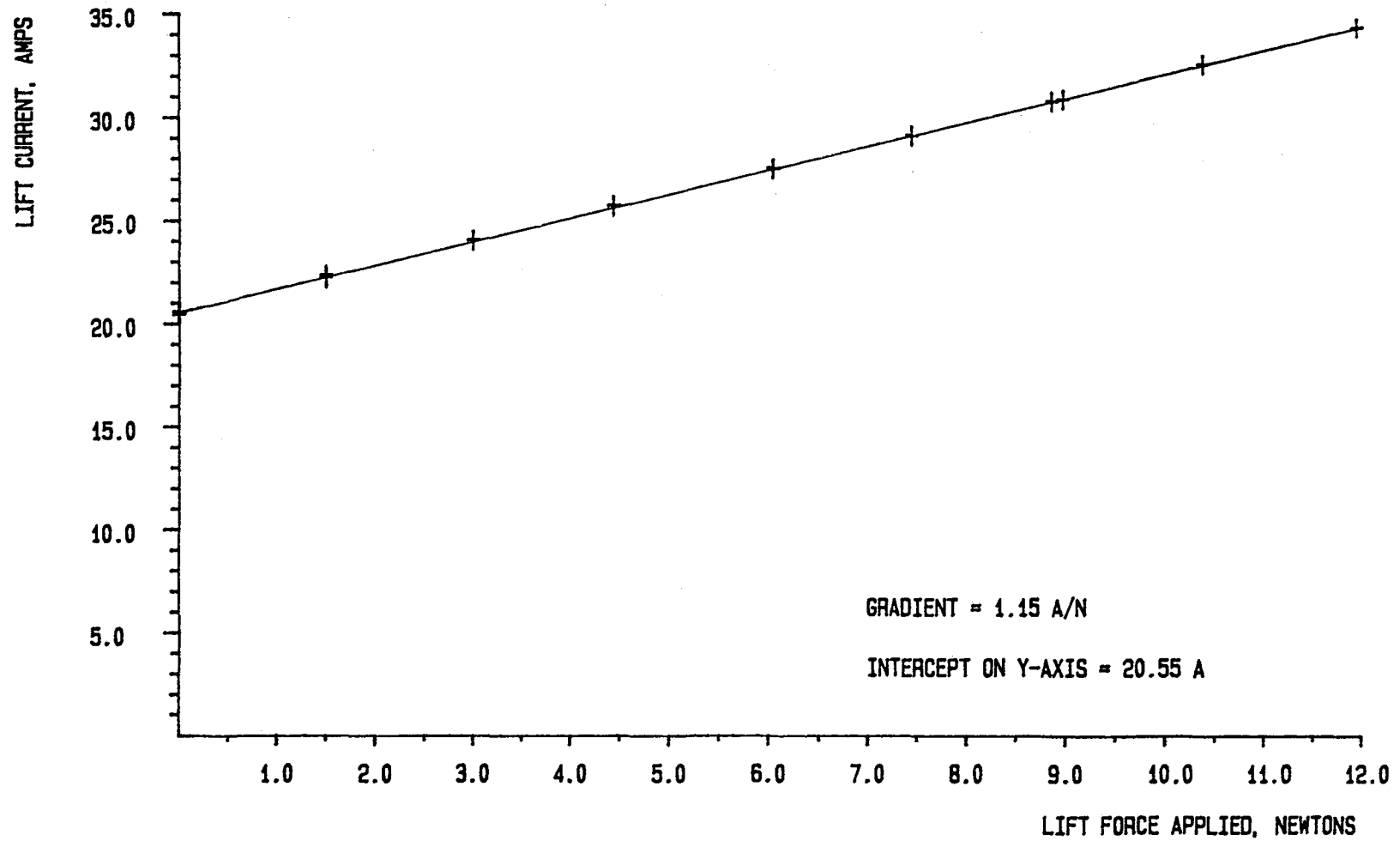
Fig.5   STATIC DRAG CALIBRATION OF THE SUPERCONDUCTING MODEL AT A SOLENOID CURRENT OF 15A

GRADIENT =   .537   A/N

INTERCEPT ON Y-AXIS =   2.79E-02   A
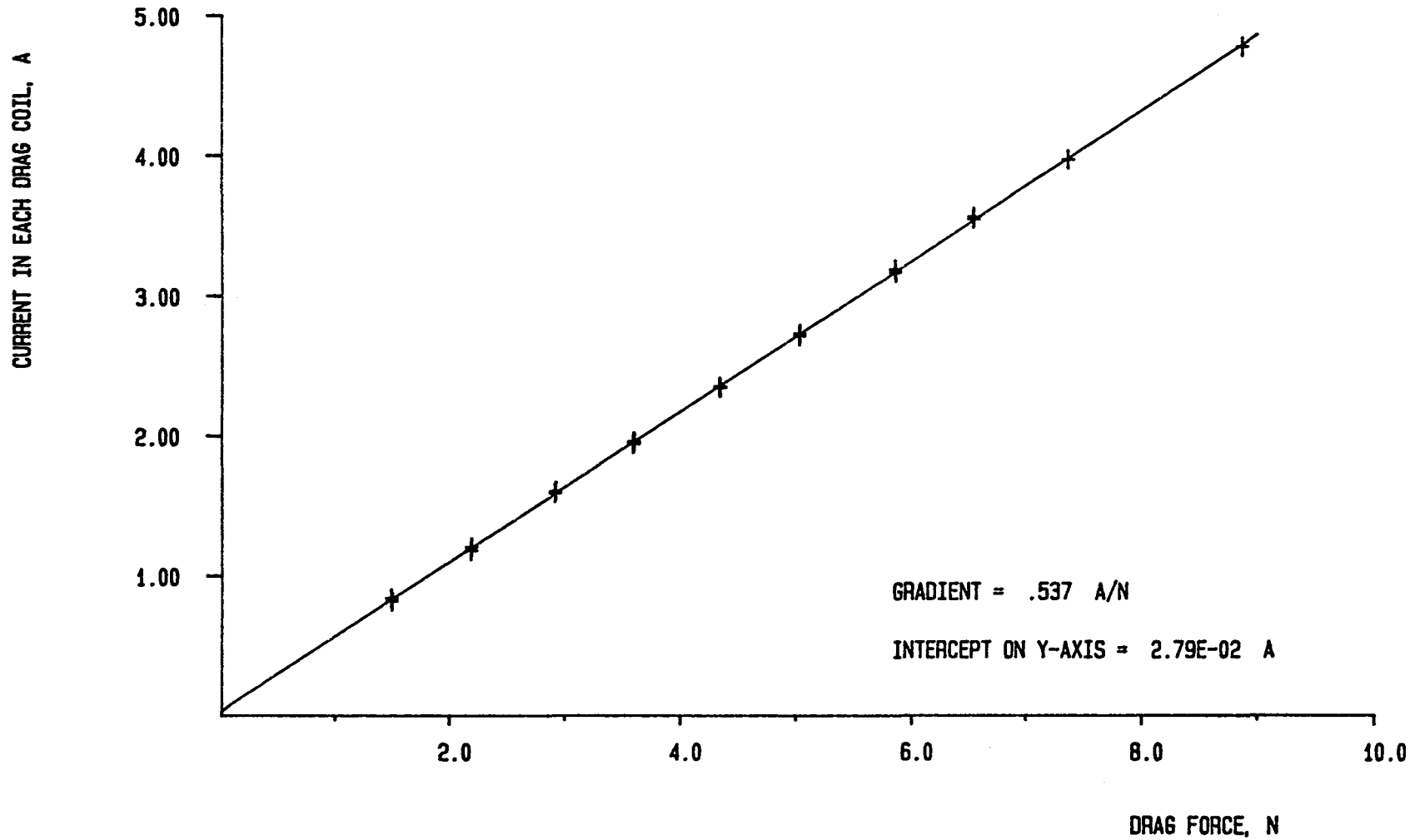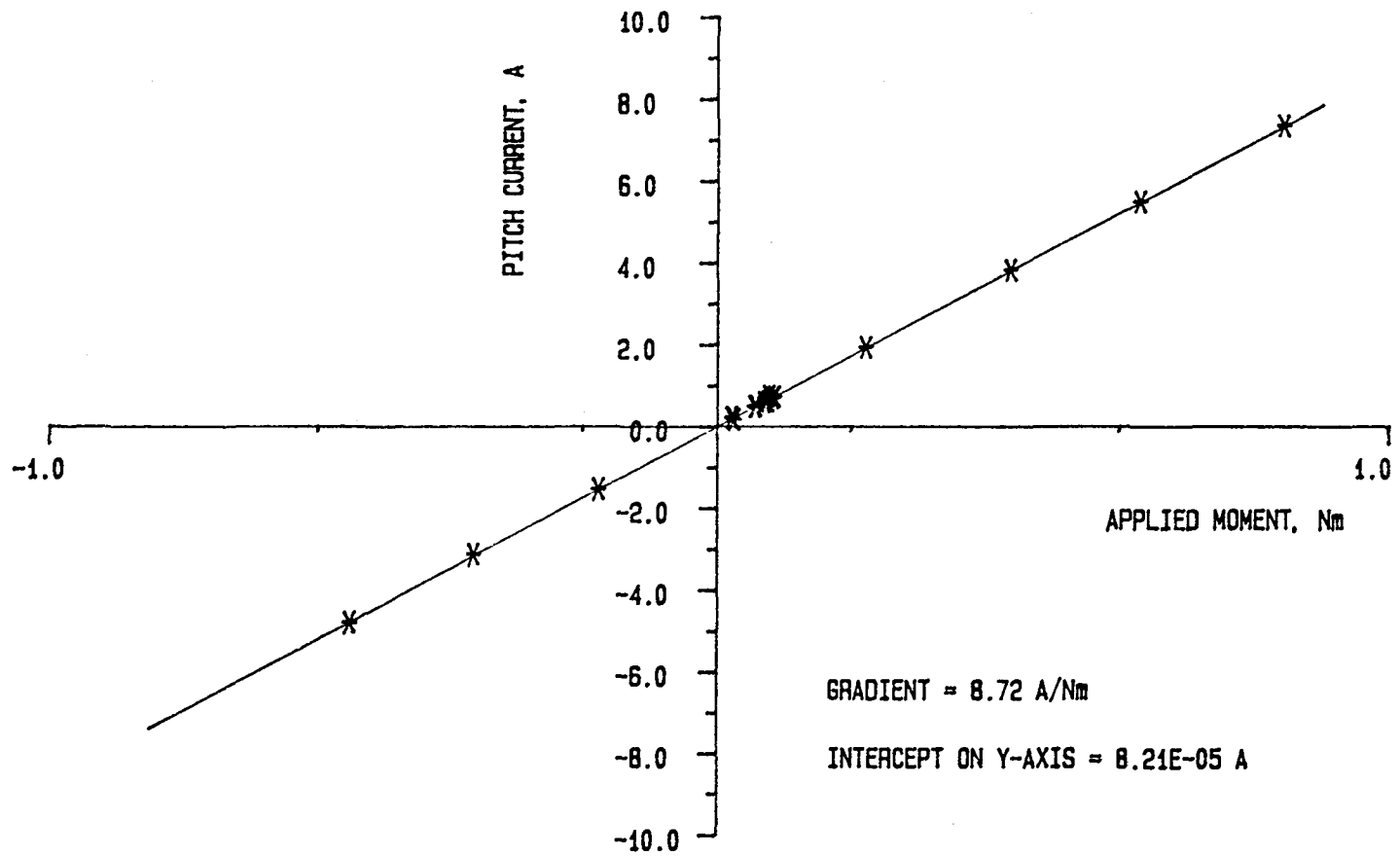
Fig.6   PITCH MOMENT CALIBRATION (SOLENOID CURRENT @15A)
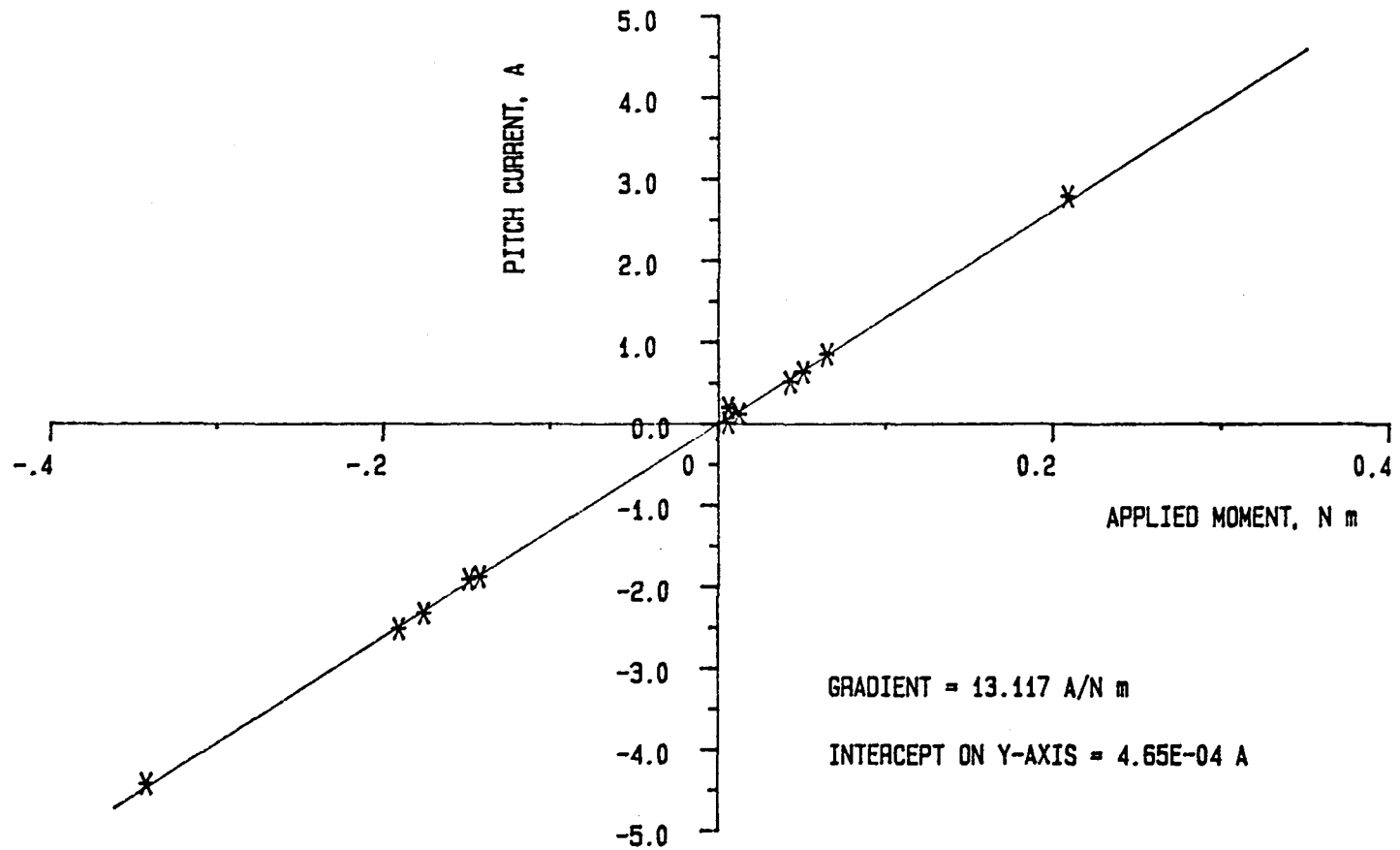
Fig.7 PITCH MOMENT CALIBRATION (SOLENOID CURRENT @10A)

Fig.8 VARIATION OF LIFT CONSTANT WITH SUPER-CONDUCTING SOLENOID CURRENT

GRADIENT = 8.34 E-02

INTERCEPT ON Y-AXIS = 3.94 E-02
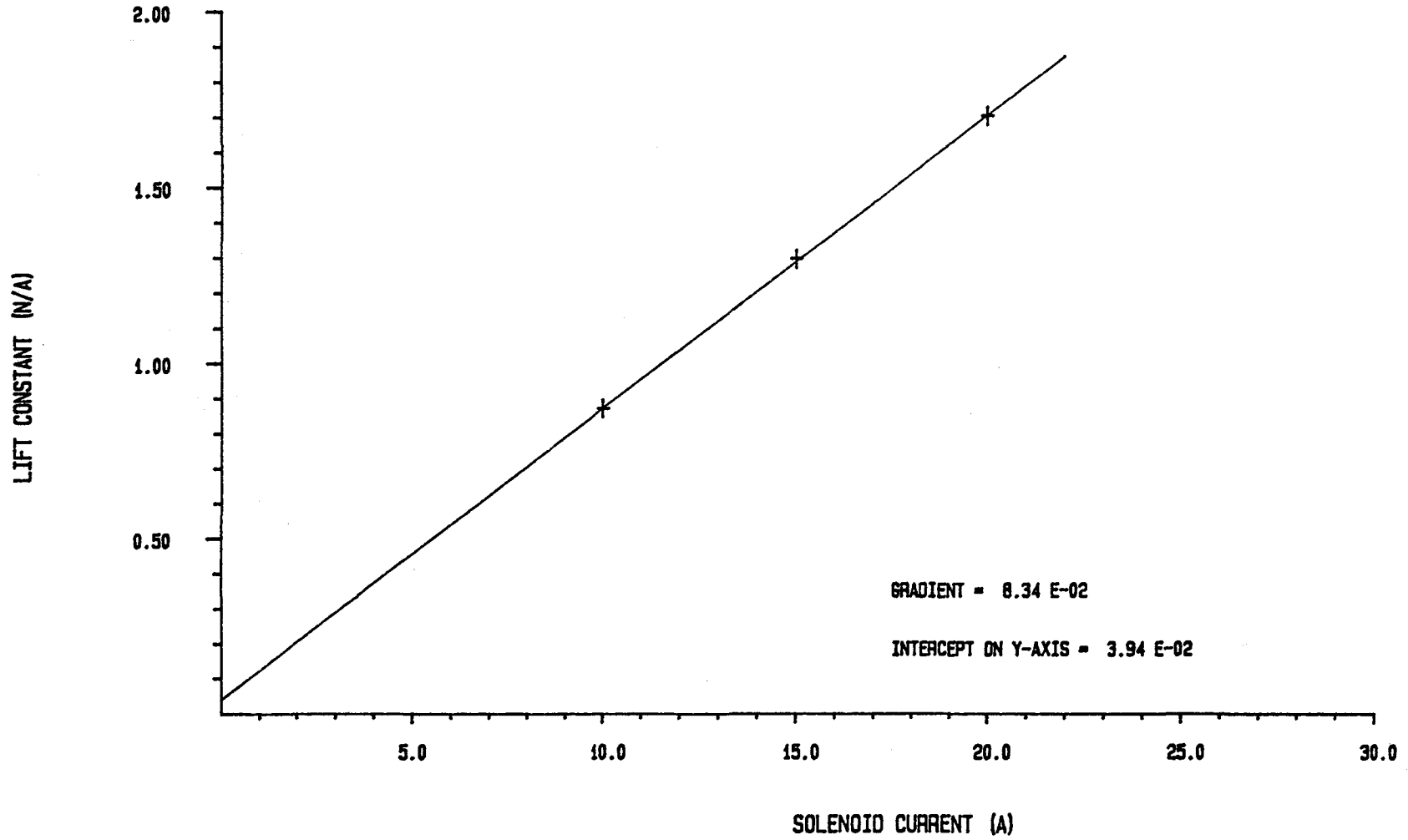
Fig.9 VERTICAL LIGHT SENSOR CALIBRATION

23
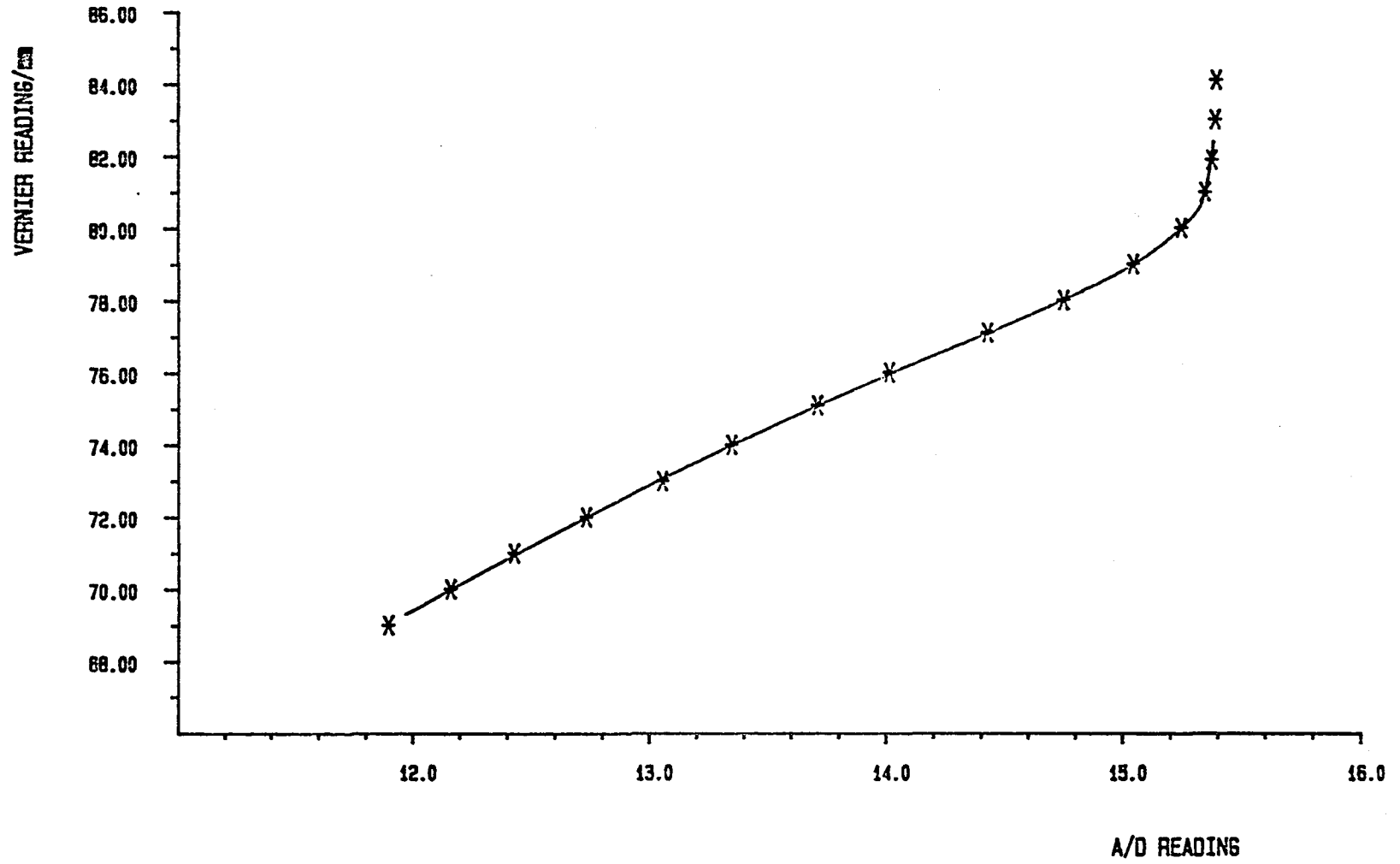
Fig. 10 DYNAMIC LIFT OSCILLATION — SUPERCONDUCTING MODEL   (SOLENOID CURRENT=15A, FREQUENCY=34.5 RAD/S
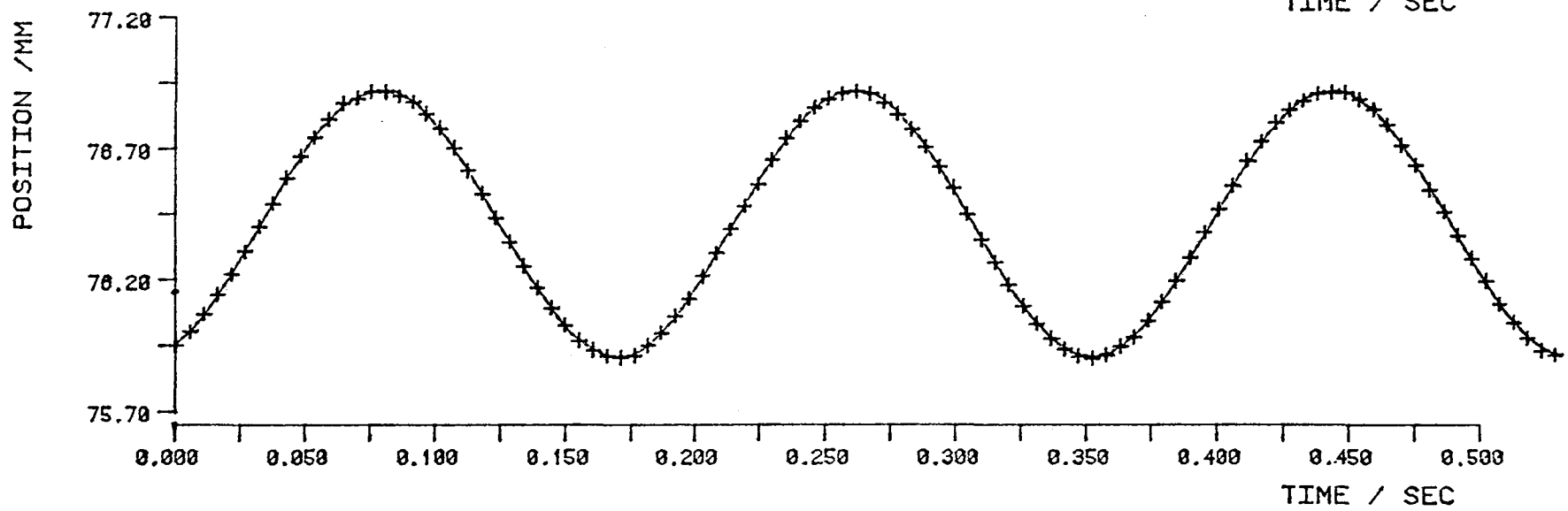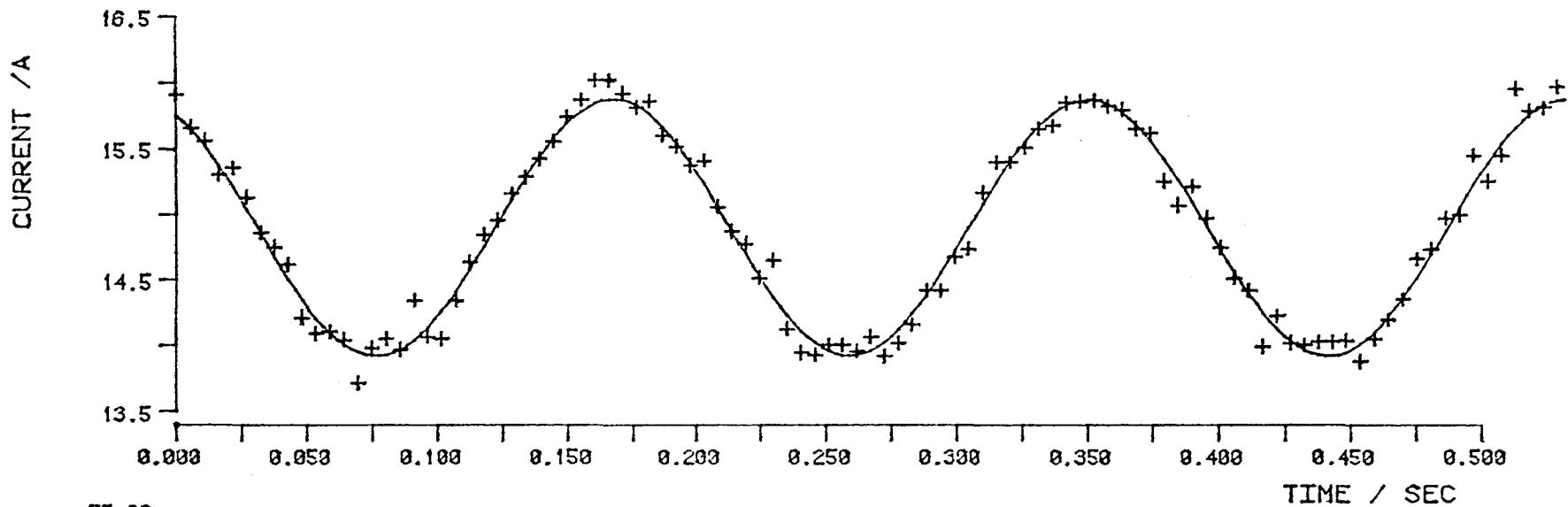
Fig. 11   DYNAMIC LIFT OSCILLATION - SUPERCONDUCTING MODEL   (SOLENOID CURRENT=15A, FREQUENCY=73.5 RAD/S)
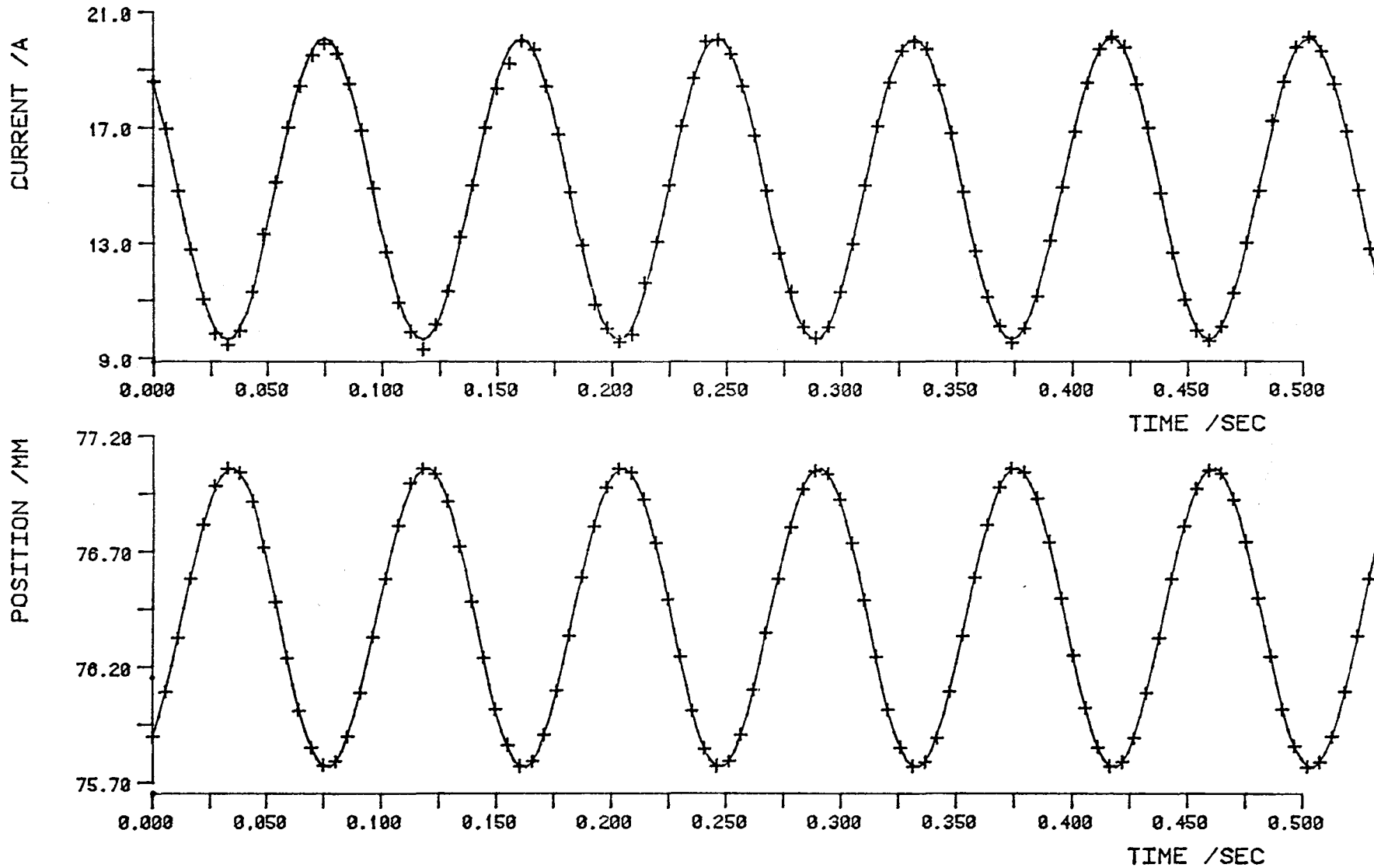
Fig.12 DYNAMIC LIFT OSCILLATION — SUPERCONDUCTING MODEL (SOLENOID CURRENT=15A, FREQUENCY=101.2 RAD/S)
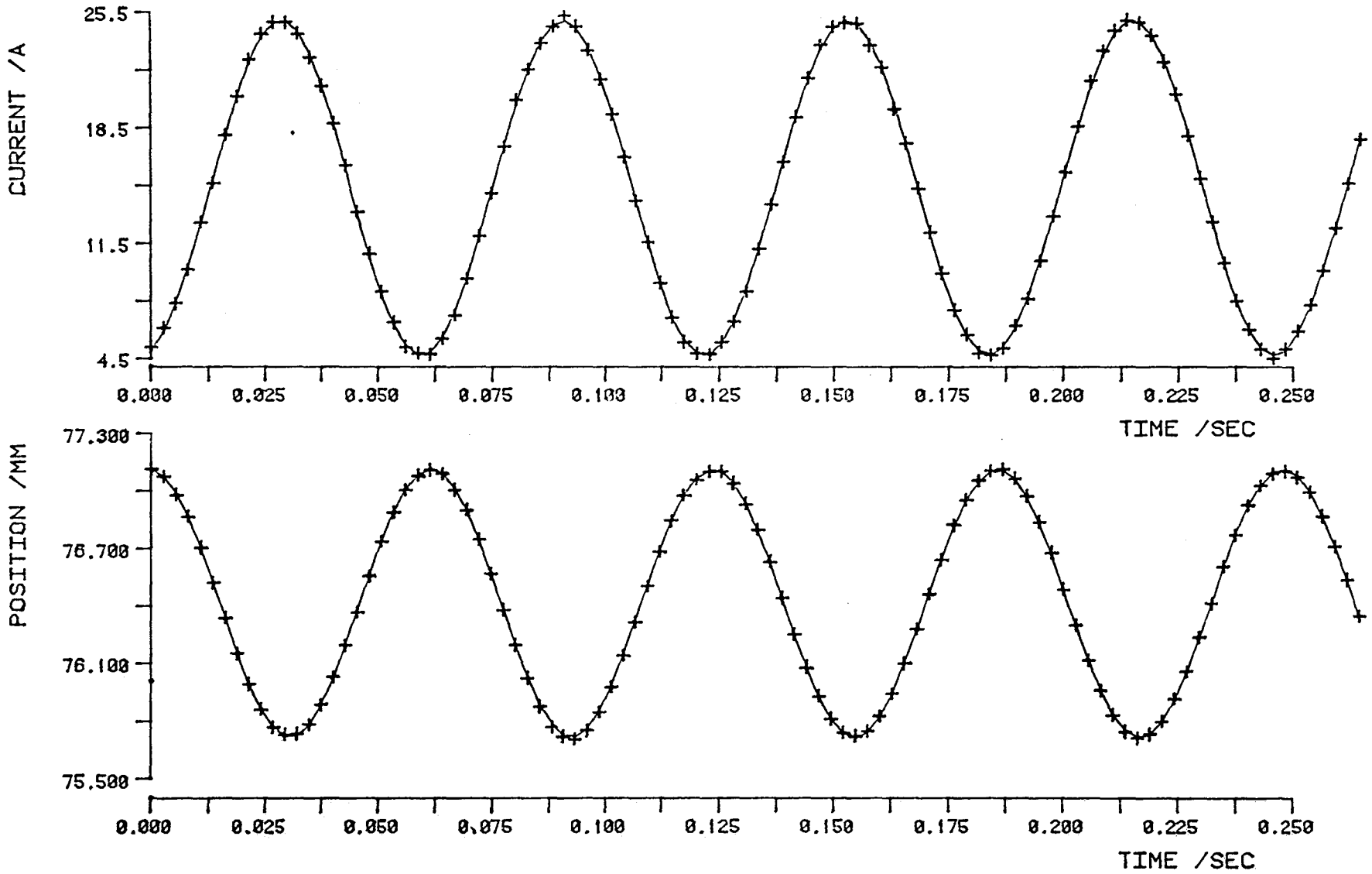
Fig.13 DYNAMIC LIFT OSCILLATION – SUPERCONDUCTING MODEL (SOLENOID CURRENT=10A, FREQUENCY=101.1 RAD/S)
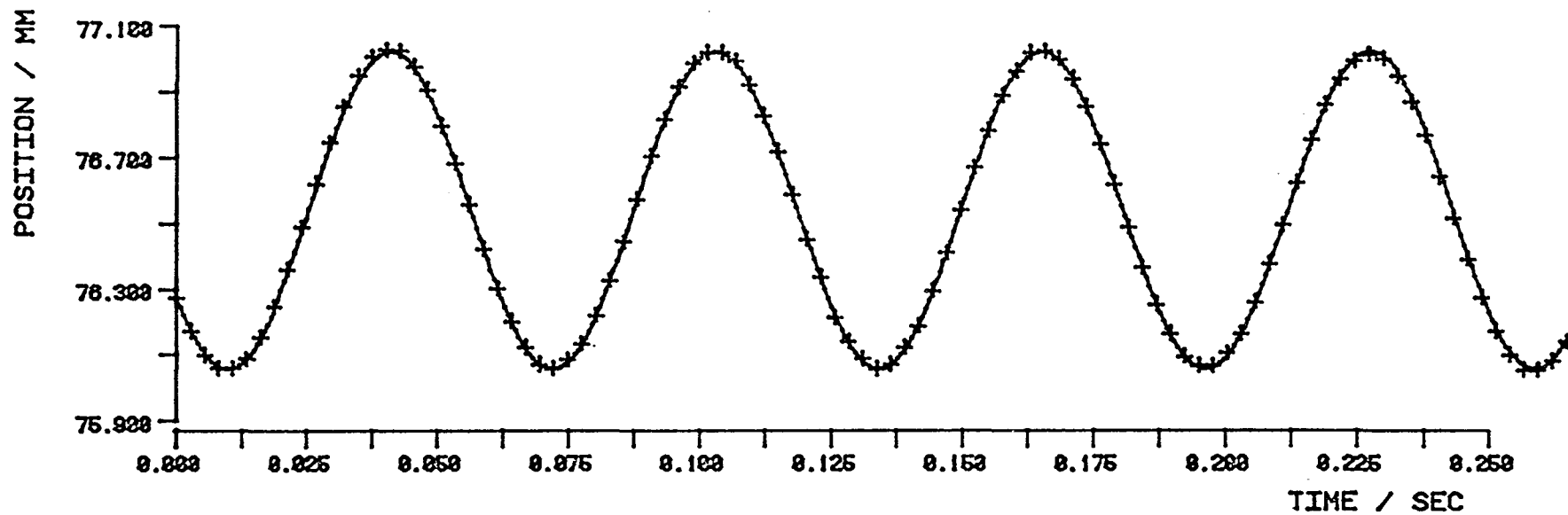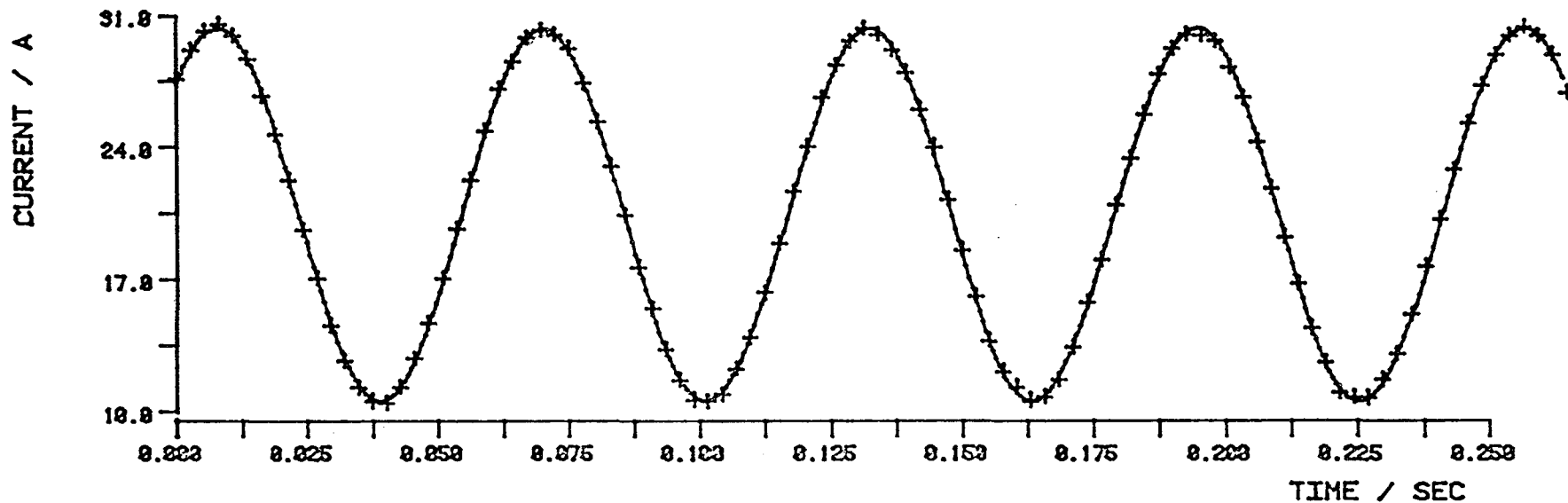
Fig. 14   DYNAMIC LIFT OSCILLATION – SUPERCONDUCTING MODEL   (SOLENOID CURRENT=20A, FREQUENCY=101.1 RAD/S)
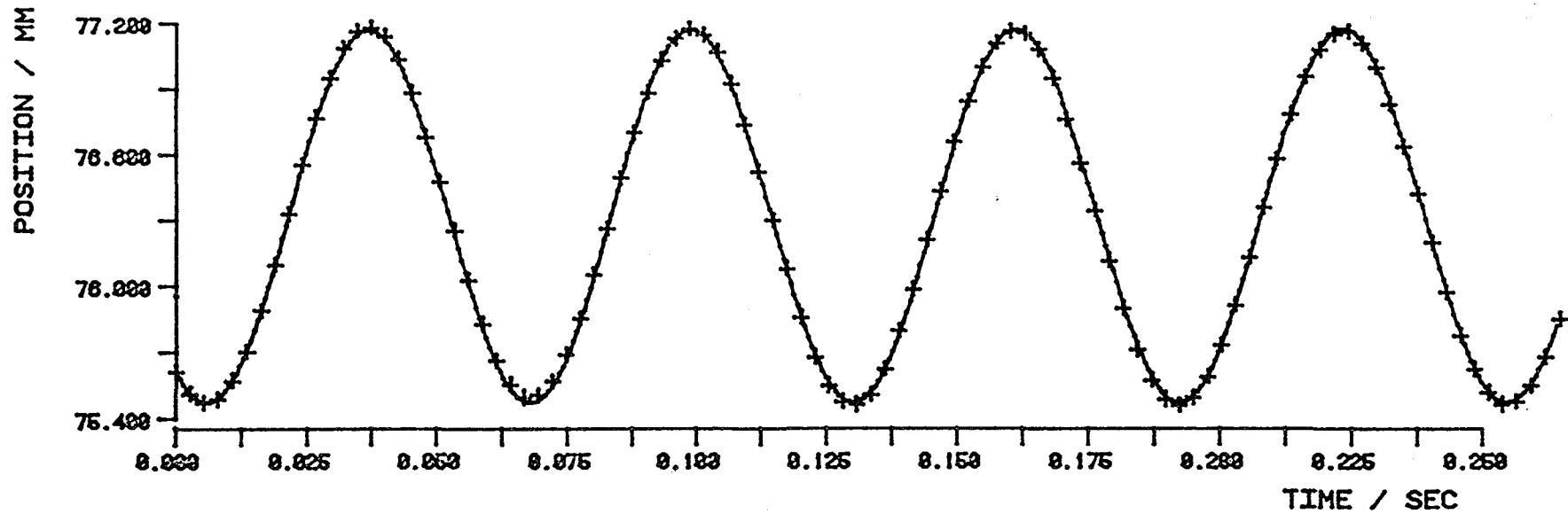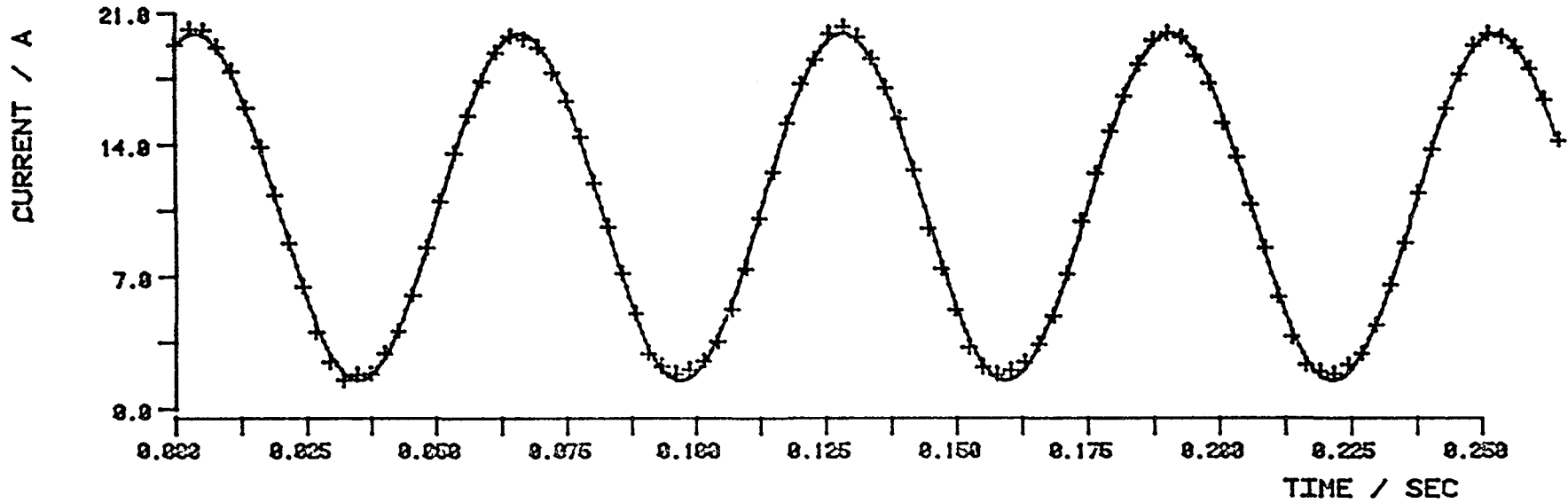
Fig. 15   DYNAMIC PITCH OSCILLATION - SUPERCONDUCTING MODEL   (SOLENOID CURRENT=15A, FREQUENCY=73.5 RAD/S)

29
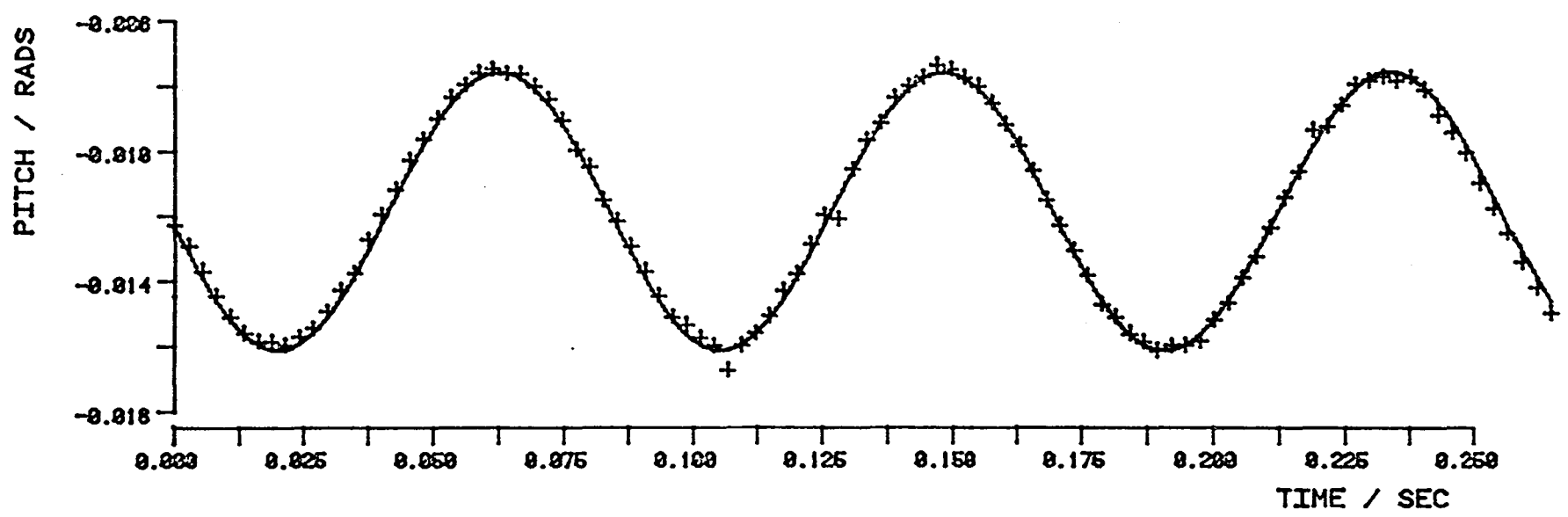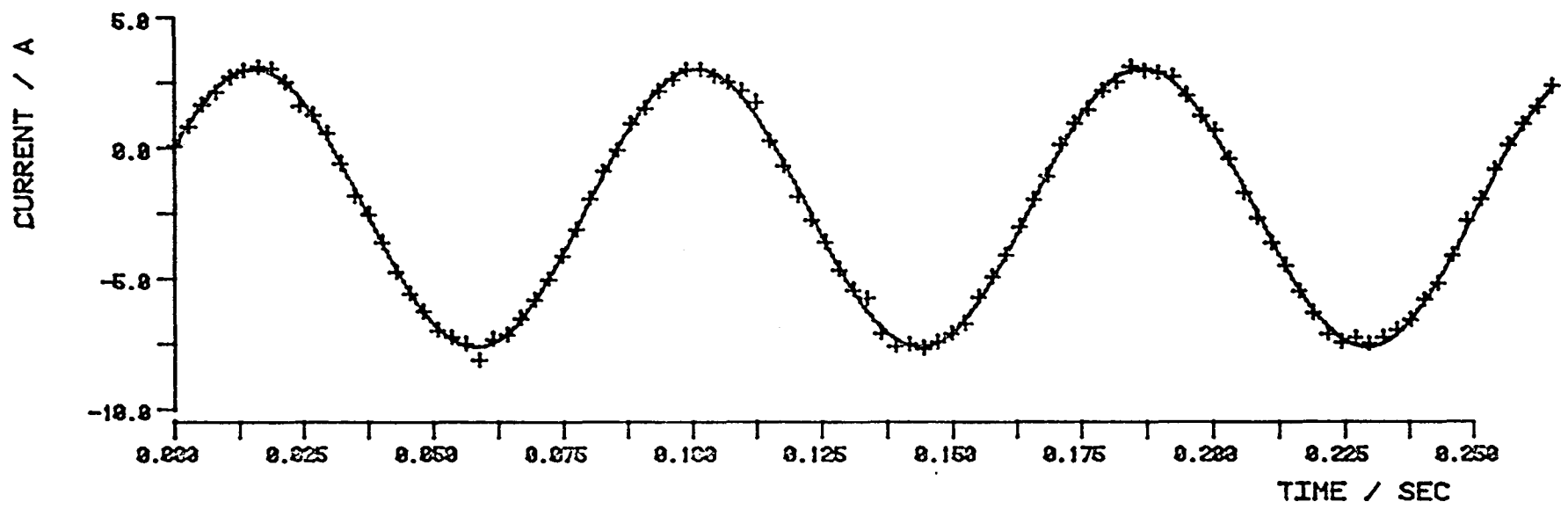
Fig. 15 DYNAMIC PITCH OSCILLATION – SUPERCONDUCTING MODEL (SOLENOID CURRENT=10A, FREQUENCY=73.6 RAD/S)
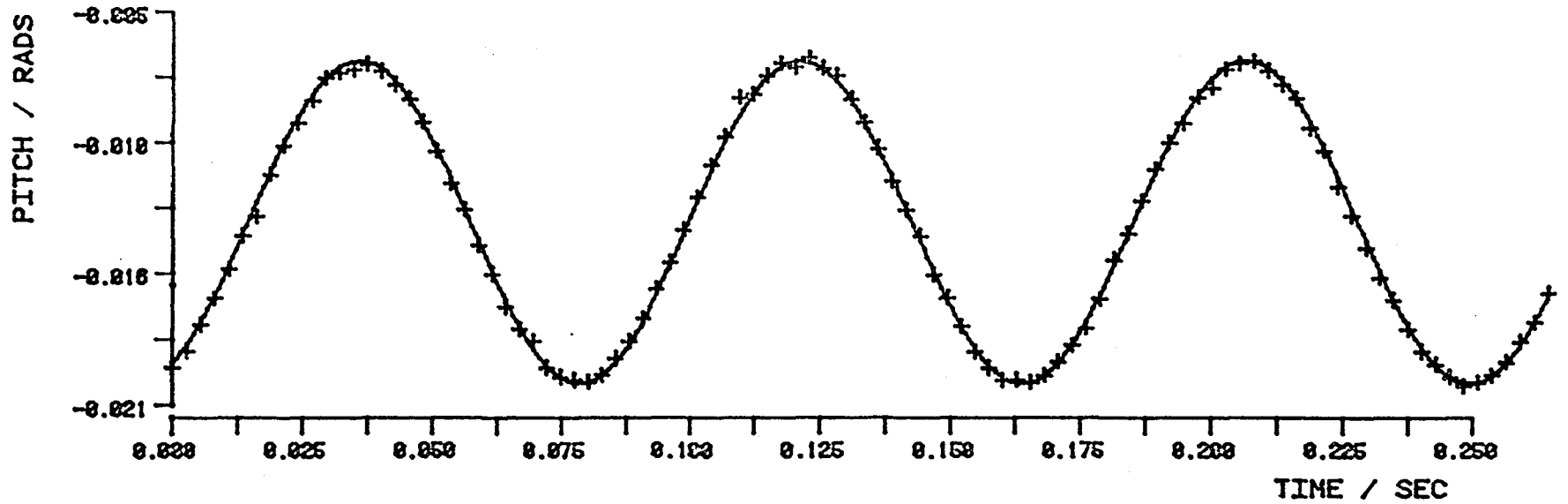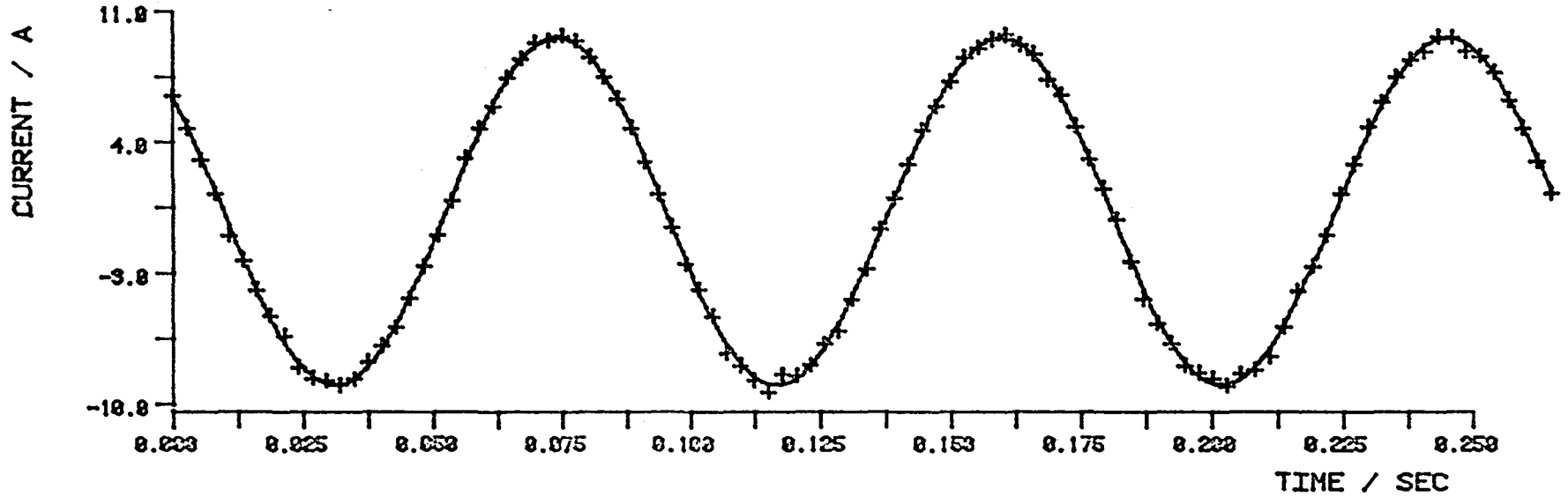
Fig. 17 STATIC LIFT CALIBRATION OF ALNICO MODEL

GRADIENT = 13.58 A/N

INTERCEPT ON Y-AXIS = 24.59 A
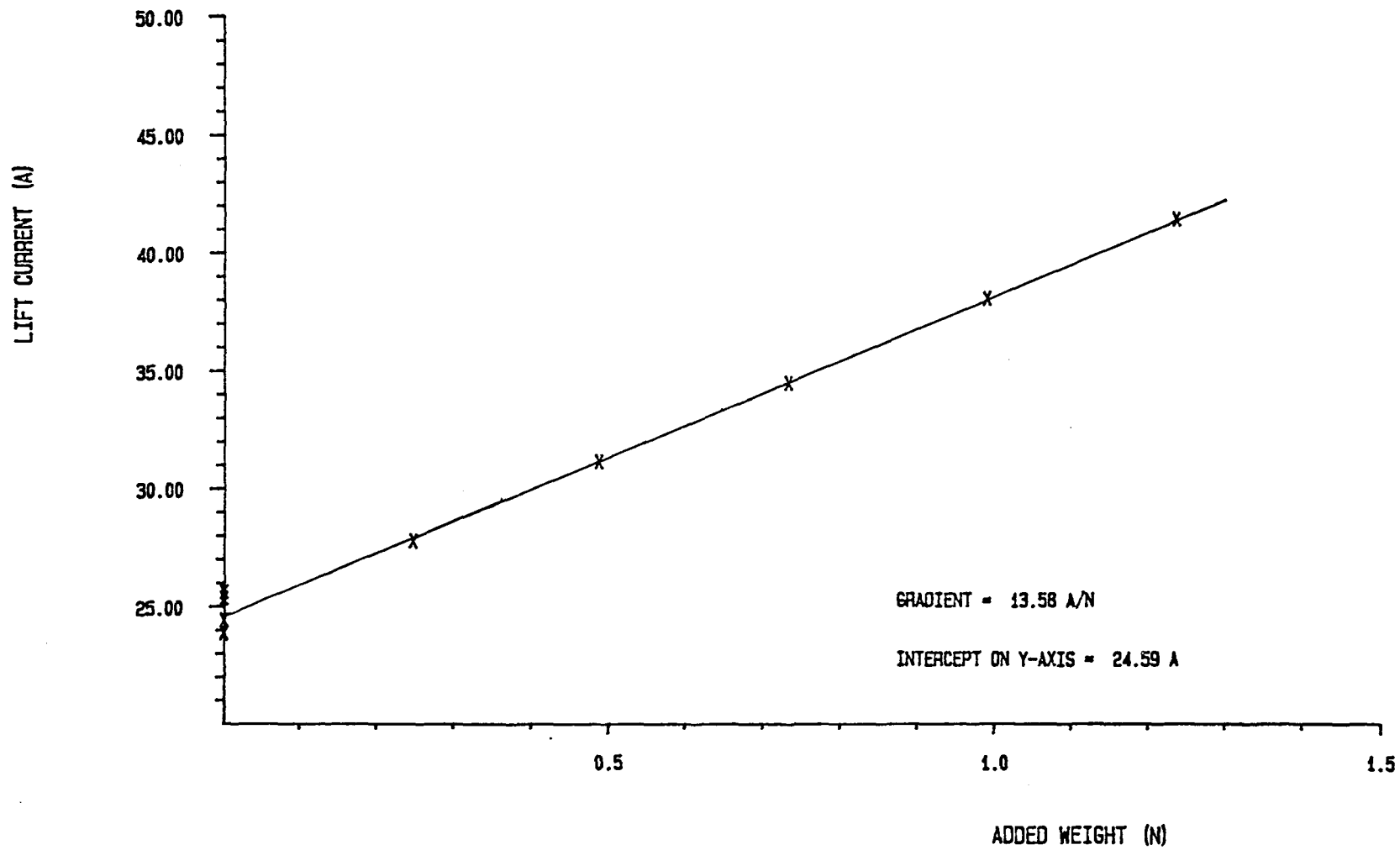
Fig.18 STATIC CALIBRATION OF SAMARIUM-COBALT MODEL

GRADIENT = 18.33 A/N

INTERCEPT ON Y-AXIS = 32.99 A
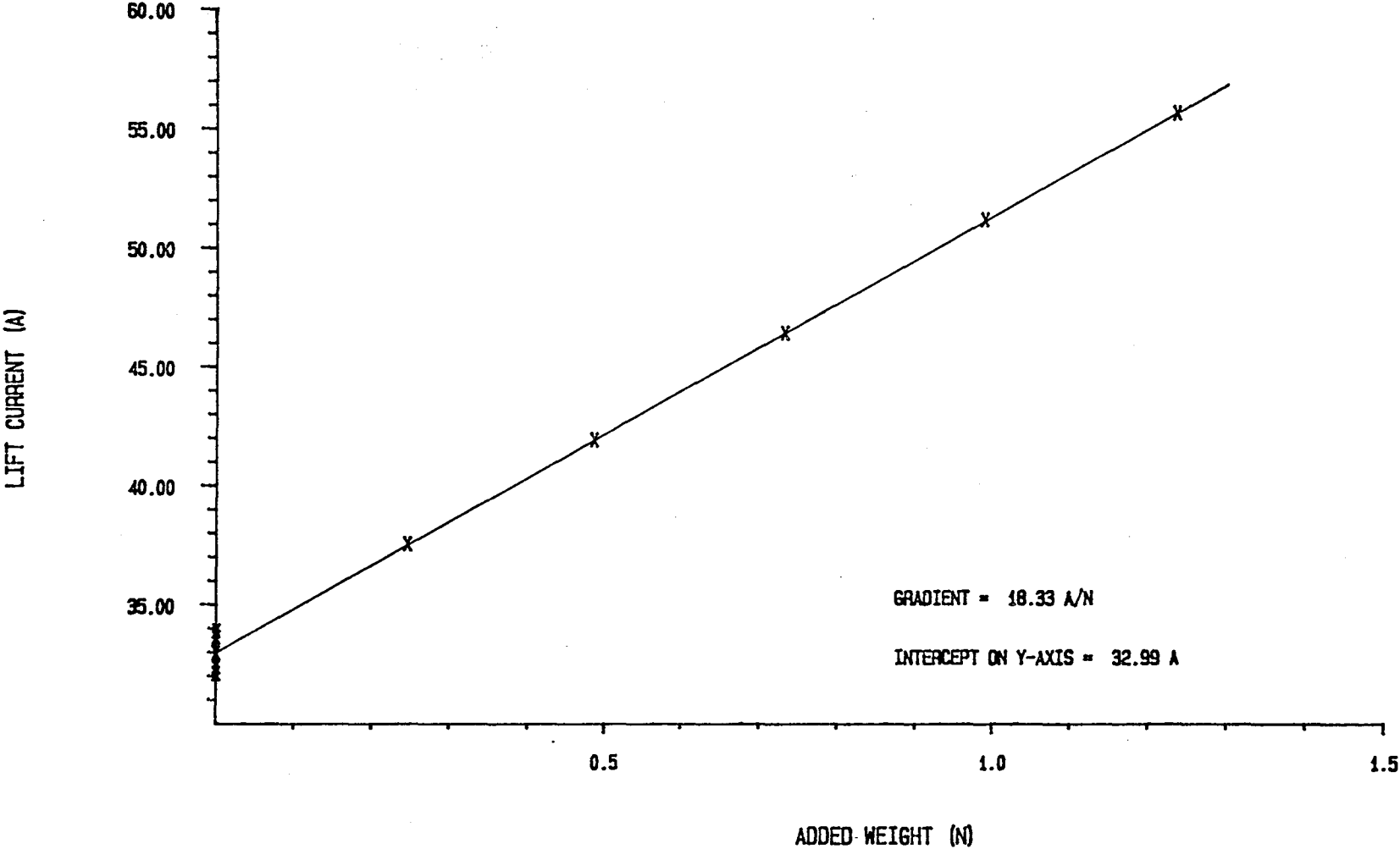
Fig.19   DYNAMIC LIFT OSCILLATION - ALNICO MODEL   (FREQUENCY=46.0 RAD/S)
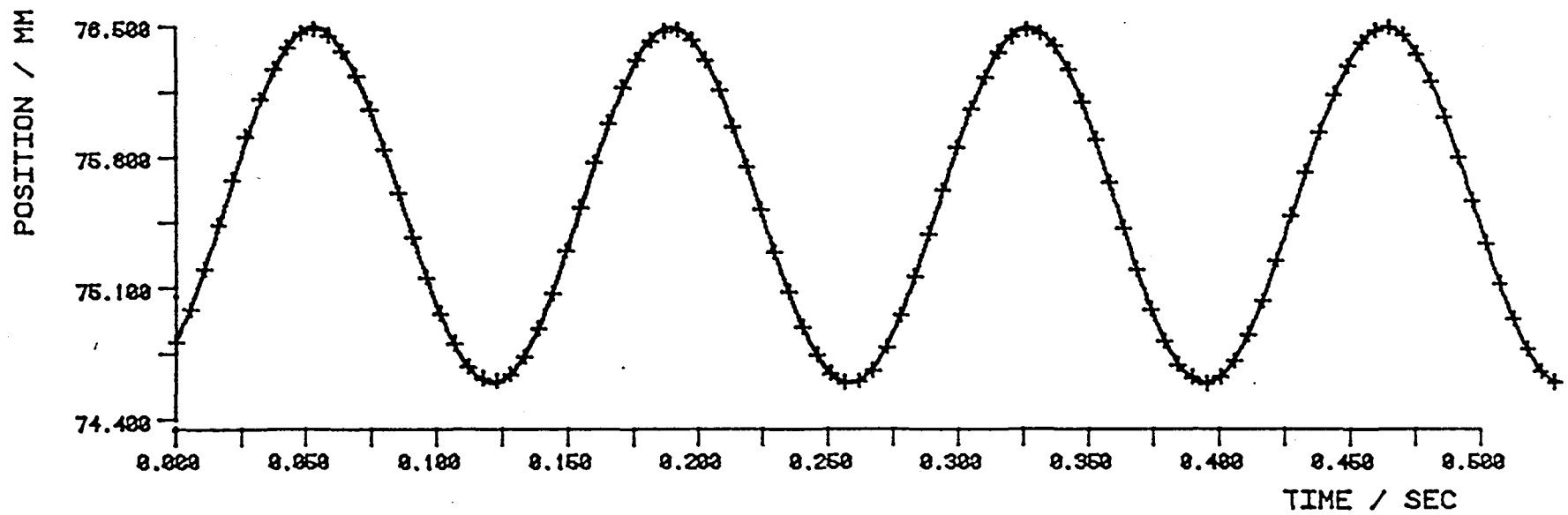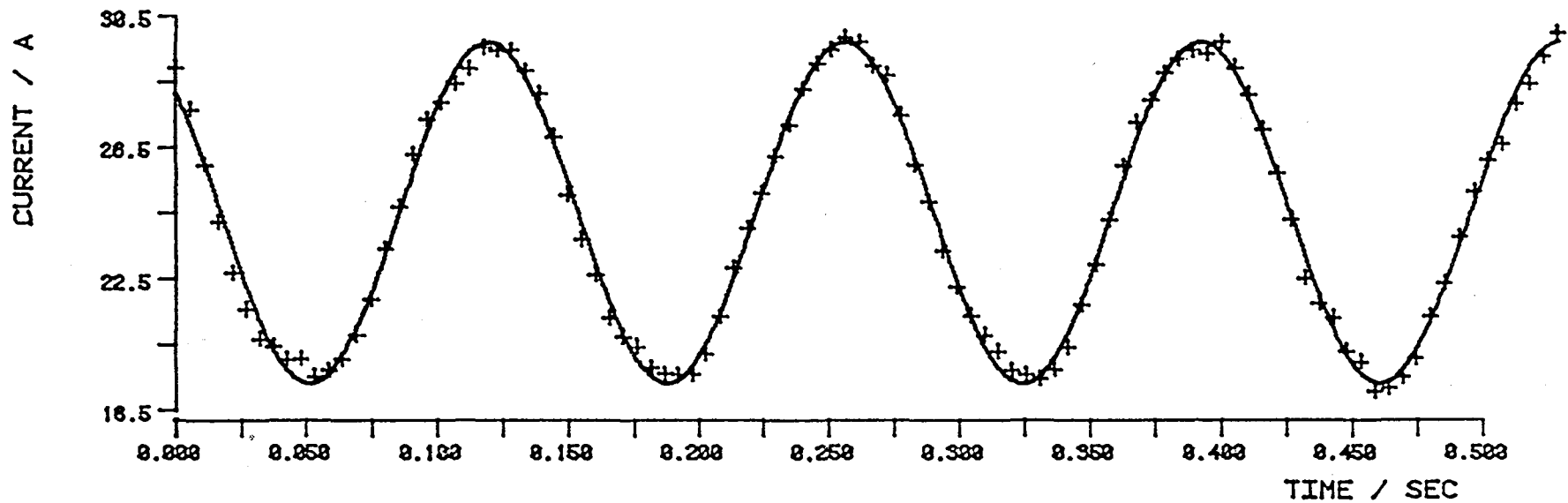
Fig.20   DYNAMIC LIFT OSCILLATION — ALNICO MODEL   (FREQUENCY=103.0 RAD/S)
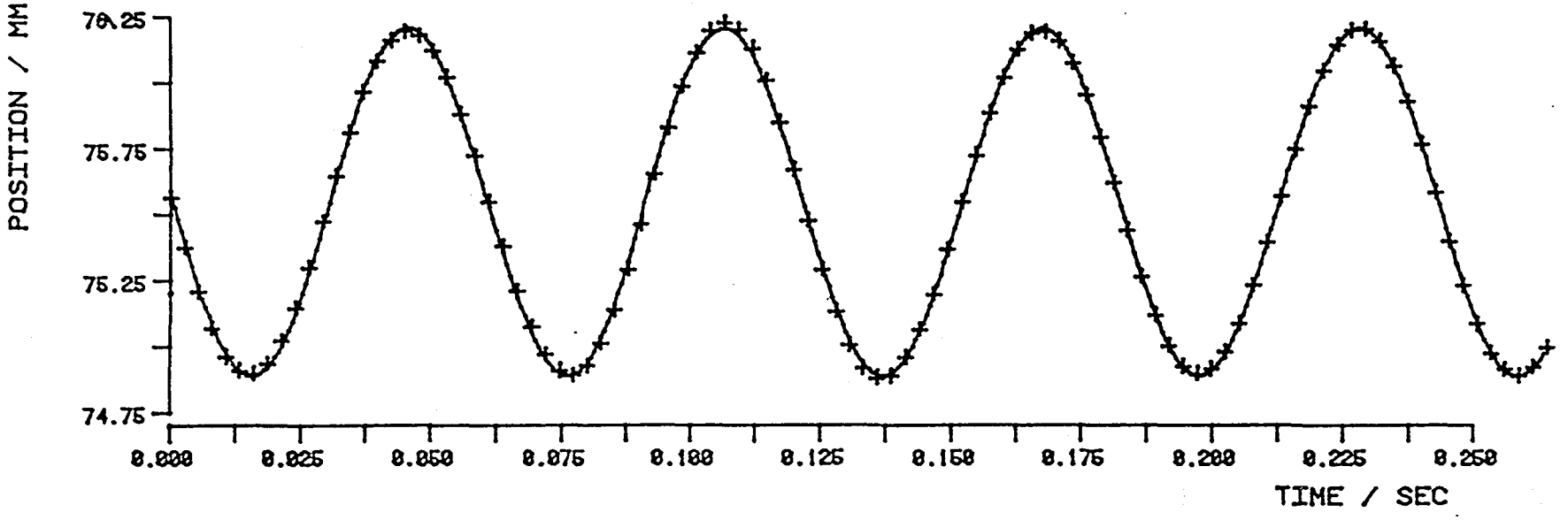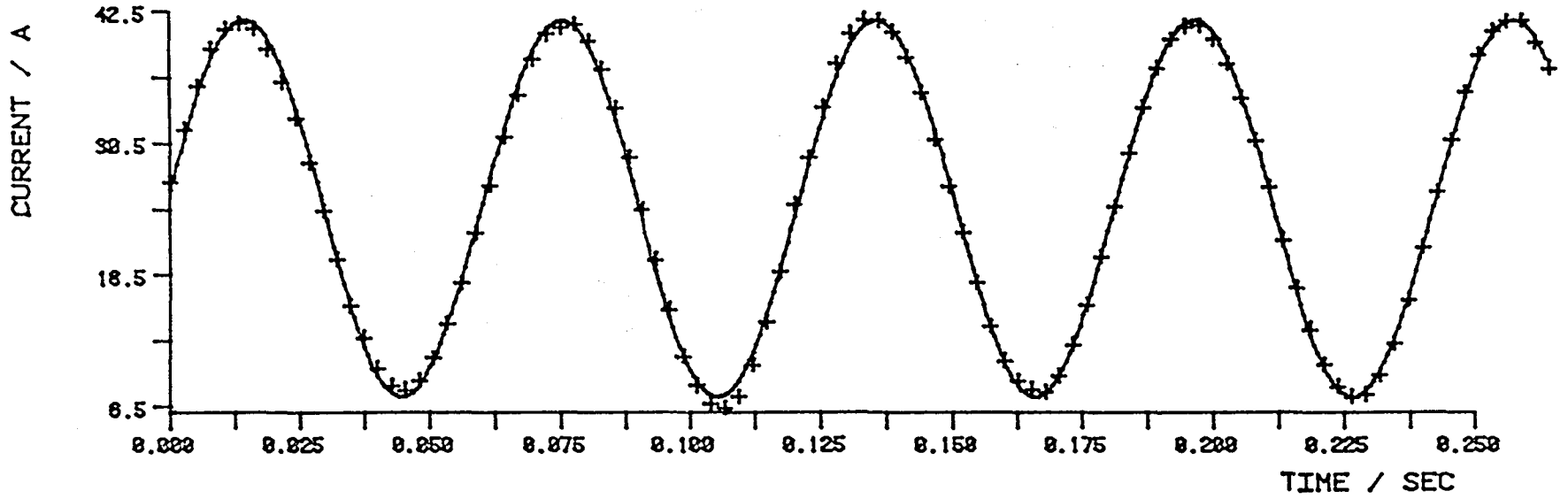
Fig.21   DYNAMIC LIFT OSCILLATION - SAMARIUM-COBALT MODEL   (FREQUENCY=45.9 RAD/S)
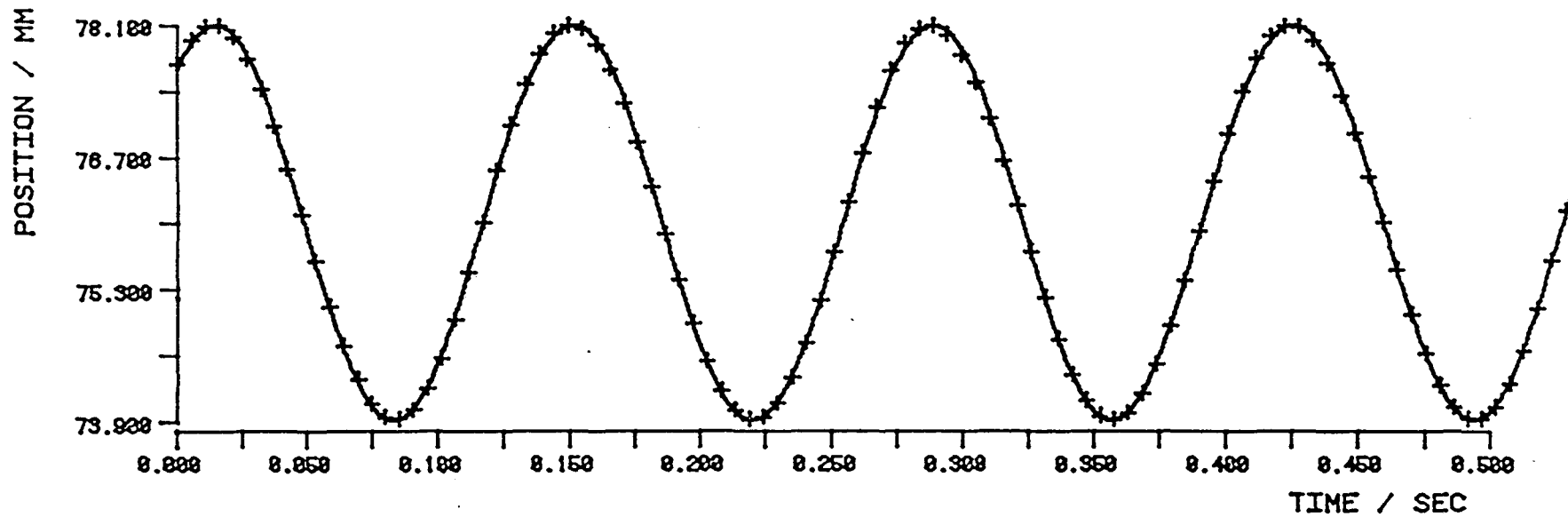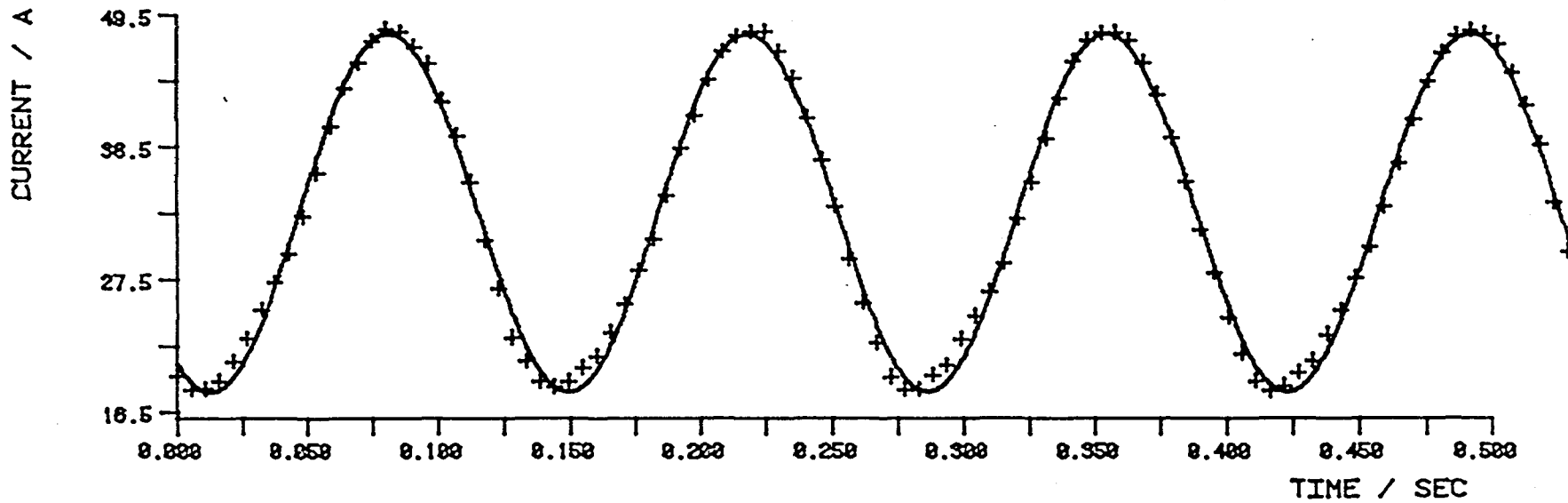
Fig.22   DYNAMIC LIFT OSCILLATION - SAMARIUM-COBALT MODEL   (FREQUENCY=108.0 RAD/S)
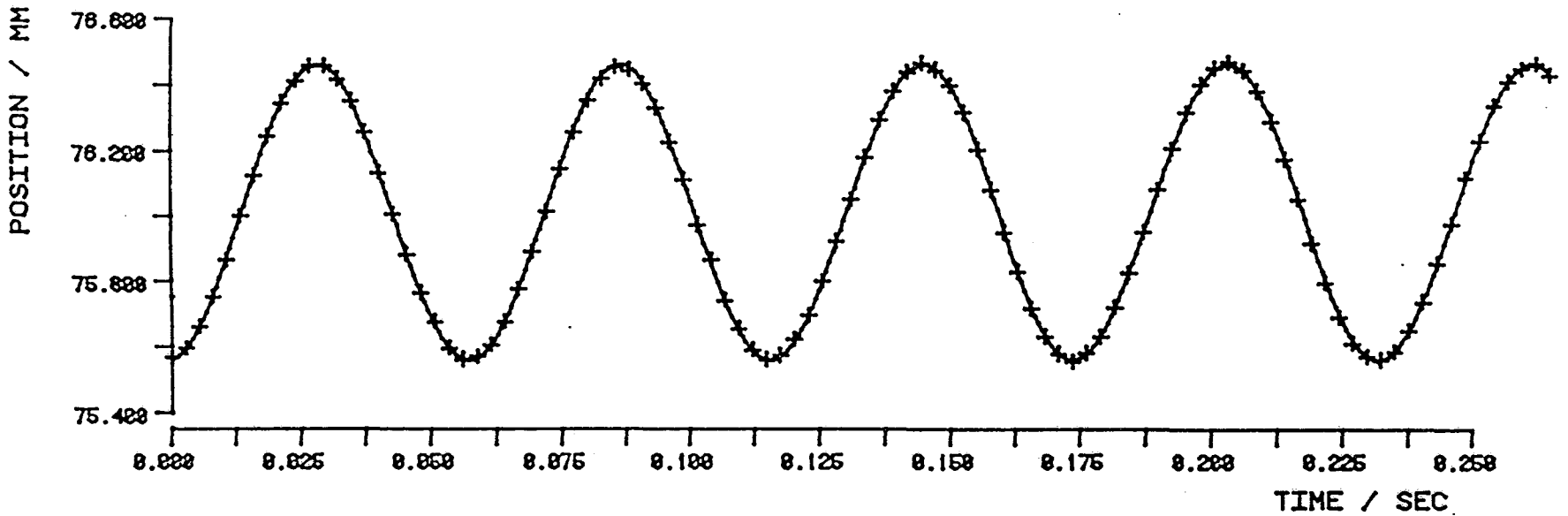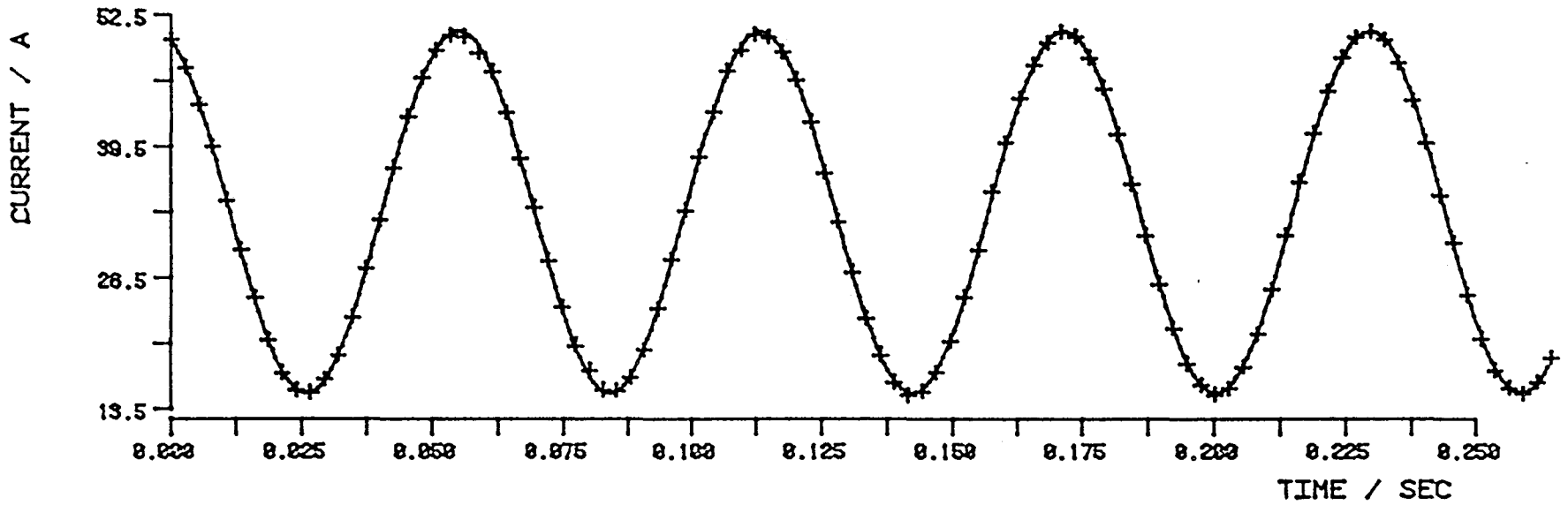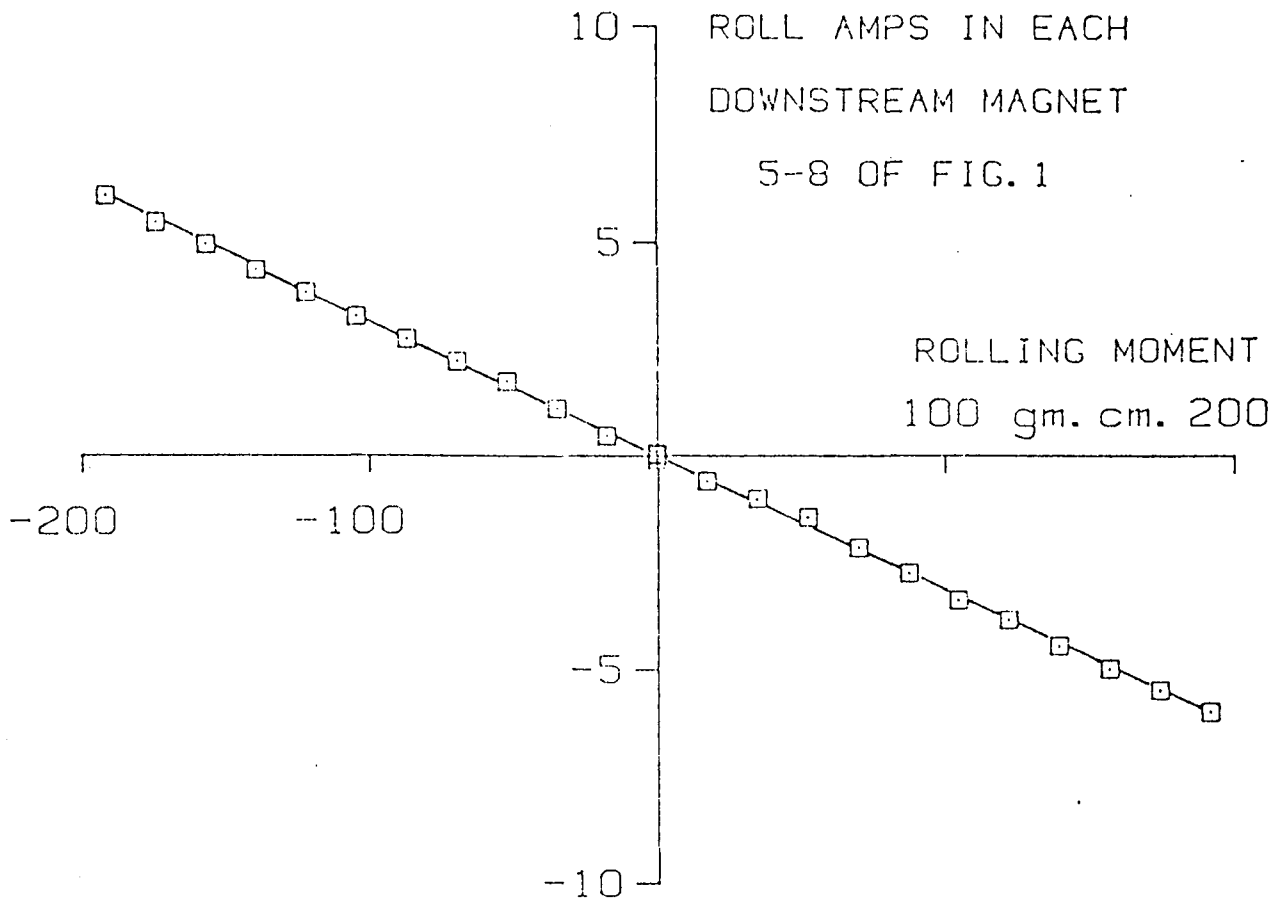
Fig. 23   CALIBRATION OF THE SAMARIUM-COBALT ROLLING MOMENT ELEMENT
MOUNTED ON THE SUPERCONDUCTING MODEL

Fig.24 ANALYSIS OF DYNAMIC LIFT CALIBRATION DATA FOR THE SUPERCONDUCTING MODEL

38
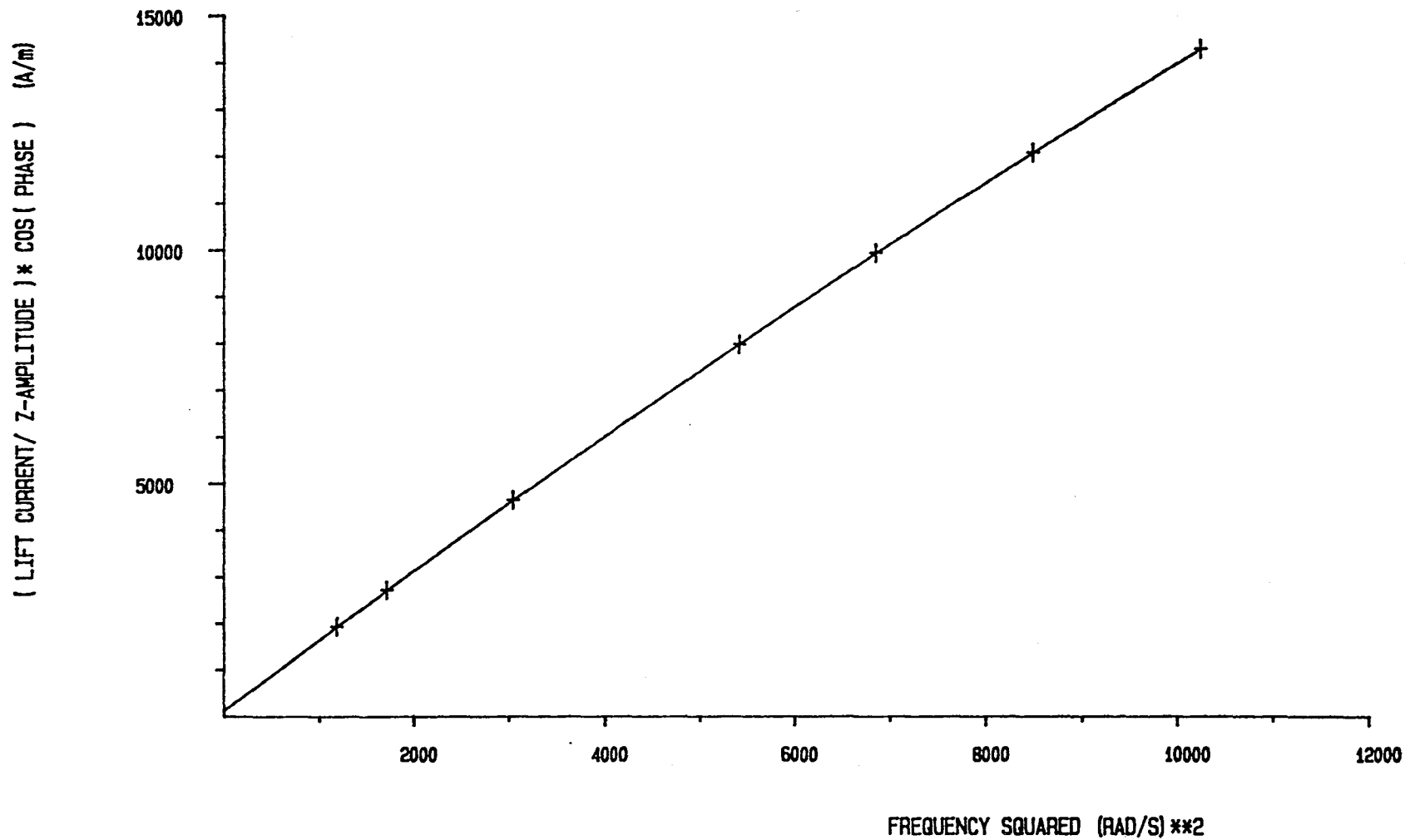
Fig. 25   ANALYSIS OF DYNAMIC LIFT CALIBRATION DATA FOR AN ALNICO MODEL

39
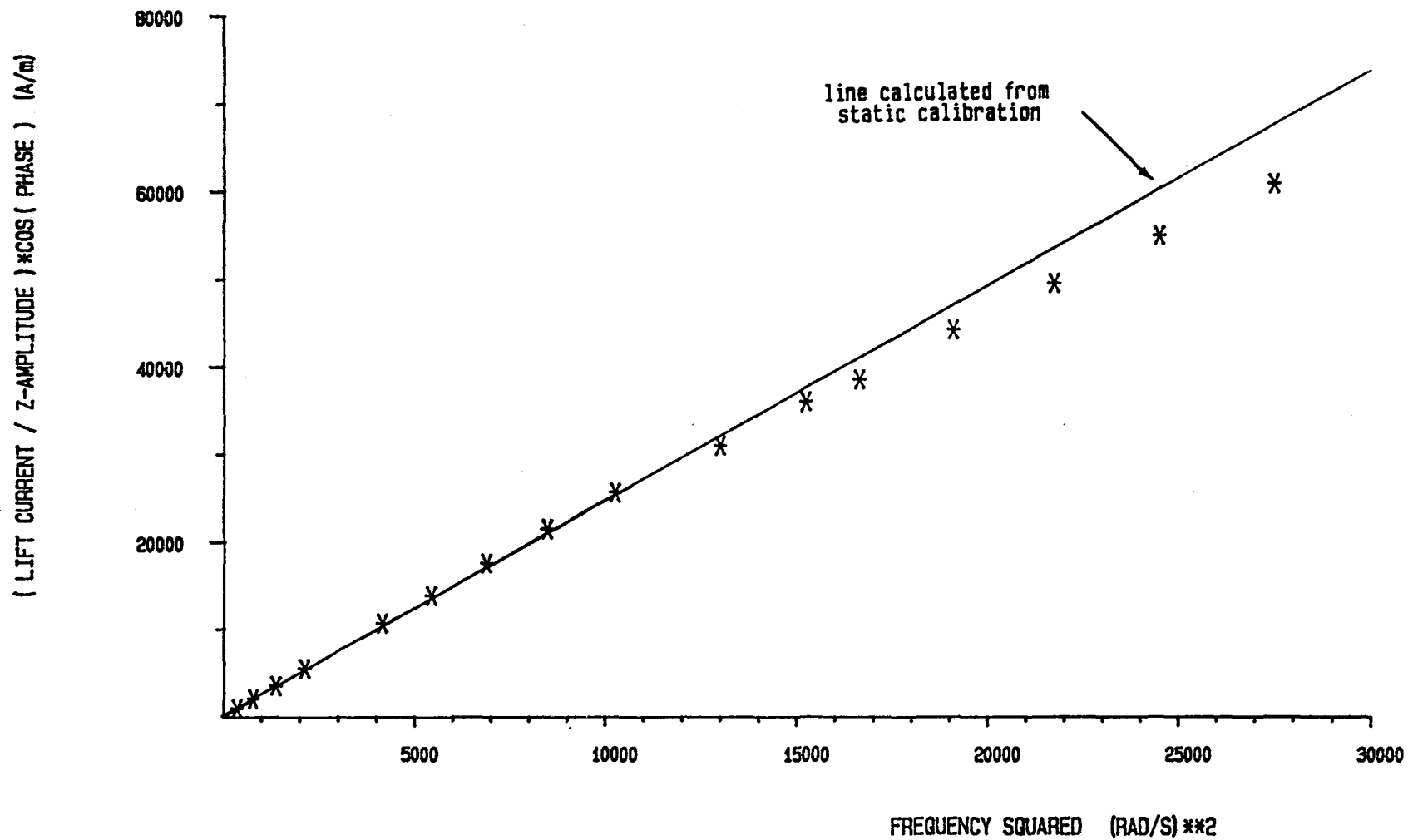
Fig.26 ANALYSIS OF DYNAMIC LIFT CALIBRATION FOR A SAMARIUM-COBALT MODEL

line calculated from
static calibration

FREQUENCY SQUARED   (RAD/S)**2

(LIFT CURRENT / Z-AMPLITUDE)*COS(PHASE)   (A/m)

40
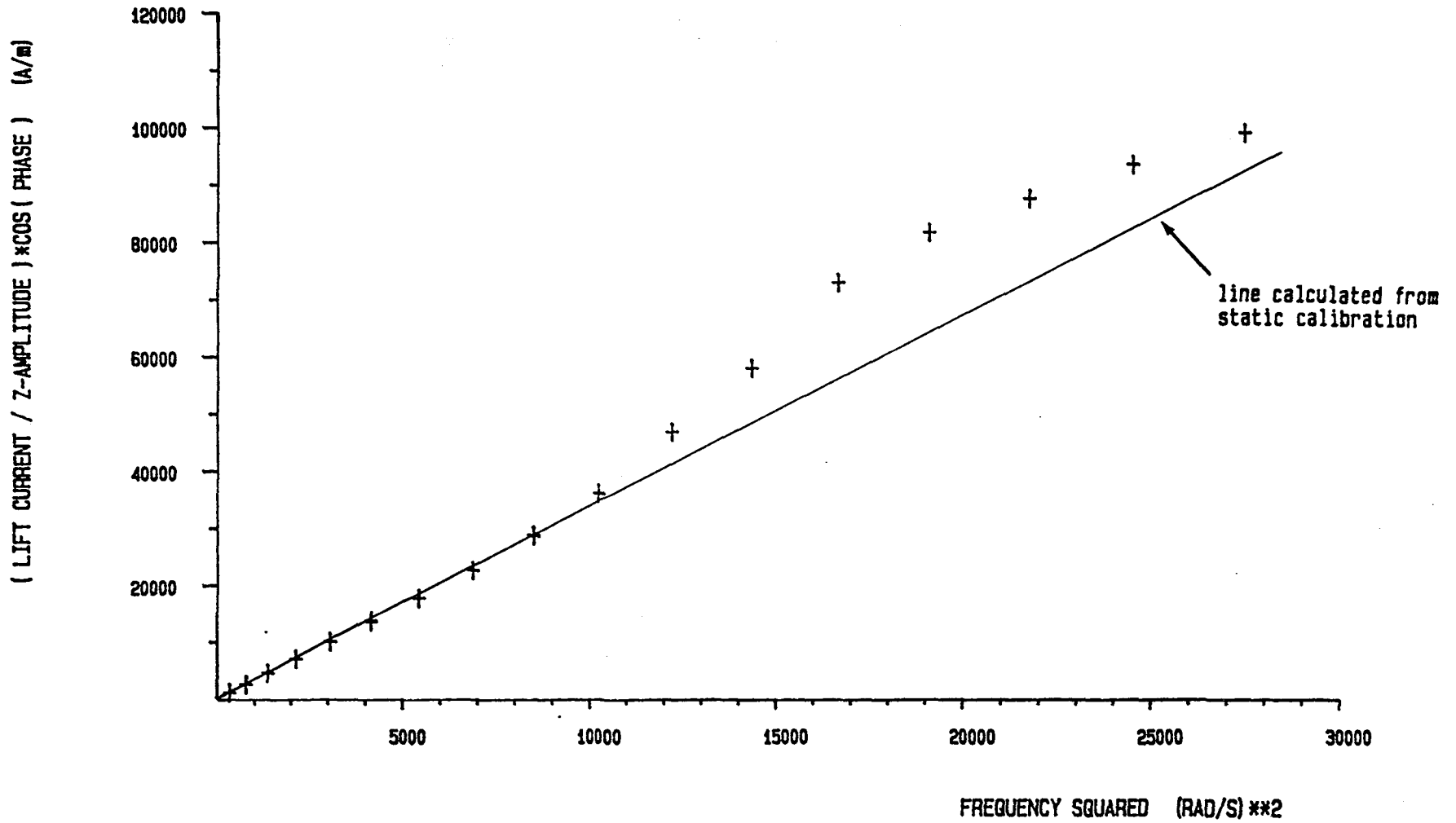
Fig.27 ANALYSIS OF DYNAMIC PITCH CALIBRATION FOR THE SUPERCONDUCTING MODEL

GRADIENT = .216 A*(s**2)/(RAD**3)

INTERCEPT ON Y-AXIS = 11.038 A/ RAD

1. Report No. NASA CR-178056	2. Government Accession No.	3. Recipient's Catalog No.

4. Title and Subtitle Further Investigation Into Calibration Techniques for a Magnetic Suspension and Balance System	5. Report Date February 1986
	6. Performing Organization Code

7. Author(s) J. Eskins	8. Performing Organization Report No.
	10. Work Unit No.

9. Performing Organization Name and Address University of Southampton Department of Aeronautics and Astronautics Southampton S09 5NH ENGLAND	11. Contract or Grant No. NSG-7523
	13. Type of Report and Period Covered Contractor Rpt. 1/85-9/85

12. Sponsoring Agency Name and Address National Aeronautics and Space Administration Washington, DC 20546	14. Sponsoring Agency Code 505-61-01-02

15. Supplementary Notes

Langley Technical Monitor: Richmond P. Boyden

16. Abstract

   This report details calibrations performed on three different magnetic cores for wind tunnel models suspended in the Southampton University Magnetic Suspension and Balance System (SUMSBS).

   The first core investigated was the Southampton University pilot Superconducting Solenoid model, first flown in July 1983. Static calibrations of lift force, drag force and pitching moment, together with lift force and pitching moment calibrations determined by the dynamic method are detailed in this report. Other types of core investigated in a similar manner were conventional permanent magnets, Alnico and samarium-cobalt.

   All static calibrations gave a linear dependence of force on electromagnet current as expected. Dynamic calibrations are faster to perform but are proving to be not as easily analysed as static calibrations. There are still some effects to be explained but dynamic lift calibration results were obtained agreeing to within 2 percent of the static calibration value.

17. Key Words (Suggested by Author(s)) Magnetic suspension Dynamic calibration Force calibration	18. Distribution Statement Unclassified - Unlimited Star Category - 09

19. Security Classif. (of this report) Unclassified	20. Security Classif. (of this page) Unclassified	21. No. of Pages 43	22. Price A03